

## ELECTRONIC SUPPORTING INFORMATION (ESI)

# Intensified Biocatalytic Production of Enantiomerically Pure Halophenylalanines from Acrylic Acids Using Ammonium Carbamate as the Ammonia Source

Nicholas J. Weise,<sup>a</sup> Syed T. Ahmed,<sup>a</sup> Fabio Parmeggiani,<sup>a</sup> Elina Siirola,<sup>b</sup>  
Ahir Pushpanath,<sup>b</sup> Ursula Schell<sup>b</sup> and Nicholas J. Turner<sup>\*,a</sup>

<sup>a</sup> Manchester Institute of Biotechnology & School of Chemistry, University of Manchester, 131 Princess Street, M1 7DN, Manchester, UK

<sup>b</sup> Johnson Matthey Catalysts and Chiral Technologies, 28 Cambridge Science Park, Milton Road, CB4 0FP, Cambridge, UK

<u>Table of contents</u>	<u>Page</u>
General methods .....	S2
General procedures .....	S3
Details of the optimisation of the PAL reaction conditions with NH <sub>4</sub> OH/CO <sub>2</sub> buffer .....	S5
Optimisation of the gram scale amination of <b>1b</b> with ammonium carbamate .....	S9
Calculation of E factor values .....	S10
HPLC analysis and representative traces .....	S11
Characterisation data of compounds <b>1a-j</b> and <b>4</b> .....	S15
NMR and HRMS spectra of compounds <b>1a-j</b> and <b>4</b> .....	S20
References .....	S40

\* Corresponding author. E-mail address: [nicholas.turner@manchester.ac.uk](mailto:nicholas.turner@manchester.ac.uk)

## **General methods**

Analytical grade reagents and solvents were obtained from Sigma-Aldrich, AlfaAesar or Fisher Scientific and used without further purification, unless stated otherwise.

$^1\text{H}$  and  $^{13}\text{C}$  NMR spectra were recorded on a Bruker Avance 400 spectrometer (400.1 MHz) without additional internal standard. Chemical shifts are reported as  $\delta$  in parts per million (ppm) and are calibrated against residual solvent signal.

Reverse phase HPLC was performed on an Agilent 1200 Series LC system equipped with a G1379A degasser, a G1312A binary pump, a G1329 autosampler unit, a G1316A temperature controlled column compartment and a G1315B diode array detector.

HRMS analyses were performed using an Agilent 6510 Q-TOF mass spectrometer connected to an Agilent 1200 Series LC system.

Microwave reactions were carried out in a CEM Discoverer microwave reactor using sealed reaction vessels. Maximum power output was set to 200 W and maximum pressure was set to 247 psi. All microwave reactions were conducted under stirring.

## **Experimental Section**

### **General procedures**

#### **Preparation of the lyophilised biocatalyst**

A pET-16b expression plasmid containing the His<sub>6</sub>-tagged AvPAL open reading frame was obtained as for previous studies<sup>8</sup> and transformed into *E. coli* BL21(DE3) protein production strain (New England Biolabs) according to the supplier's protocol. Expression of the gene encoding AvPAL was conducted according to previously reported methods.<sup>8</sup> The cell mass was isolated via centrifugation, flash frozen in liquid nitrogen and freeze dried using a standard laboratory lyophiliser for 16-24 h. The dry cell mass was then ground into a fine powder and stored at -20°C until required.

#### **Small-scale amination reactions**

The powdered biocatalyst was used directly as stored by resuspending in 1-4 mL of the desired general buffer supplemented with the relevant substrate (or crude reaction mixture for telescopic reactions) at the concentration required. Where appropriate, negative control experiments were set up to lack the whole cell catalyst, the substrate or the ammonia source. The tube lid was then sealed and incubated at the appropriate temperature (500 rpm). After the desired reaction time a sample of the reaction was mixed with MeOH (1:1) and the catalyst and salts removed via centrifugation (3 min, 13000 rpm) in a benchtop centrifuge. 0.5 mL of the supernatant was prepared for analysis of the soluble fraction of the reaction through the use of a Thomson 0.45 µm PVDF filter vial. Analysis of the insoluble fraction was enabled by resuspending the pellet in borate buffer (0.1 M, pH 12.0) and repeating the centrifugation and filtration steps as before. Crude isolation of the product was performed by heating 1 mL of the supernatant at 60°C for 6 h.

#### **Intensified gram-scale amination of 3-fluorocinnamate 1b**

Larger biotransformations were performed in a 100 mL round-bottom flask positioned by a clamp and stand over a stirrer hot plate with heating block and magnetic stirrer bar. For the optimised synthesis of (S)-2b, ammonium carbamate (5.3 g), 1b (1.0 g, 6 mmol) and lyophilised biocatalyst (1.0 g) were added to water (17 mL) in the flask. Stirring was continued at 30°C for 6 h. Results were analysed by mixing a sample (100 µL) with MeOH (900 µL) and preparing as before.

### **Knoevenagel-Doebner condensation for telescopic synthesis of (S)-2b from 3**

The Knoevenagel-Doebner condensation of malonic acid and **3** was performed as described in a previous report.<sup>S1</sup> Aldehyde **3** (0.5 mmol), malonic acid (1.0 mmol) and piperidine (0.01 mmol) were dissolved in DMSO (500  $\mu$ L) and the mixture was heated in a microwave reactor (30 min, 60°C). After cooling, samples of the mixture were added to ammonium carbamate solution (4 M, pH 9.9) in different v/v ratios (10%, 20%, 30%), followed by the suitable quantity of lyophilised biocatalyst (400 mg mL<sup>-1</sup> dry cell weight). The suspension was stirred at 30°C for several hours, monitoring the conversion by HPLC.

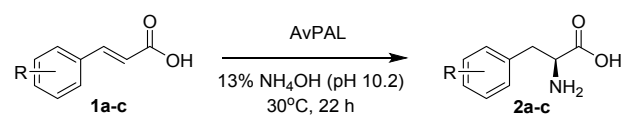
### **Chemo-enzymatic synthesis of biarylalanine (S)-4 from 1j**

The AvPAL-catalysed amination of 3-bromocinnamate **1j** was performed in a total volume of 4 mL as for the small scale reactions (25 mM substrate, 4 M ammonium carbamate pH 9.9, 30°C, 200 rpm, 24 h). HPLC analyses revealed 96% conversion and an enantiomeric excess of 99% for the amino acid product (S)-**2j**. The whole cell biocatalyst was removed and the reaction buffer evaporated as described above. The crude isolate was used to perform Boc-protection and Suzuki-Miyaura coupling with phenylboronic acid.<sup>S2</sup> The crude product and CsCO<sub>3</sub> (3.0 eq) were added to deionised water (5 mL) in a microwave reactor vessel containing a magnetic stirrer bar. THF (2.5 mL) was added followed by addition of Boc<sub>2</sub>O (1.2 eq). The solution was microwave heated (200 W, 90°C) for 15 min and cooled to room temperature. Phenylboronic acid (1.5 eq) and Pd(MeCN)<sub>2</sub>Cl<sub>2</sub> (10 mol%) were added to the reaction vessel and the mixture was microwave heated (200 W, 120°C) for 20 min. The reaction was cooled to room temperature and acidified with aq. HCl (3 mL, 3 M) and extracted with EtOAc (2  $\times$  25 mL). Combined organic extracts were dried over MgSO<sub>4</sub> and concentrated under reduced pressure. The residue was purified by column chromatography to give pure (S)-**4** as a white solid (30 mg, 24% overall yield from **1j**).

### Details of the optimisation of the PAL reaction conditions with NH<sub>4</sub>OH/CO<sub>2</sub> buffer

To ensure the industrial utility of the process from the outset, attention was first turned to testing biocatalyst formulations for optimal ease of use. To this end, lyophilised *E. coli* BL21(DE3) whole cells harbouring the overproduced AvPAL were prepared. These were then used to test the activity of the biocatalyst preparation on an analytical scale using just 5 mM fluorocinnamates **1a-c** and 5 mg mL<sup>-1</sup> dry cell mass at 30°C. Downstream processing was also considered at this stage, with the reaction buffer selected so as to allow evaporation, following the reaction and removal of the catalyst, to leave a crude isolate. As such, 13% ammonium hydroxide pH adjusted to 10.2 with carbon dioxide was chosen (as done in a previous publication<sup>S3</sup>). The reaction was found to proceed to high conversion after 22 h under these parameters (Table S1).

**Table S1.** AvPAL-catalysed amination of fluorocinnamates at 5 mM concentration.



Subs.	R	Conv. [%]	ee of 2 [%]
<b>1a</b>	2-F	98	>99 (S)
<b>1b</b>	3-F	94	>99 (S)
<b>1c</b>	4-F	86	>99 (S)

As a measure of temperature dependence of the reaction, biotransformations were repeated at various incubation temperatures with the highest converted substrate **1a** (Figure S1). Whilst there was variation in final conversions achieved across the range of temperatures, none were found to rival or exceed the original value achieved with 30°C after the same time period (98%, 24 h). Time point samples taken for each temperature reveal an interplay between the initial conversion rate and biocatalyst longevity. Whilst temperatures of 55°C and 70°C gave the higher conversions than the other temperatures after 1 hour, the rates were found to decrease rapidly within the first few hours, giving final conversions of 40% and 76% respectively. A similar, though less exaggerated trend was observed at 37°C. The use of a lower temperature of 25°C mitigated the more severe losses in activity seen at high temperatures, but the lower initial rate of the reaction resulted in a final conversion of just 59%. As such the initial incubation temperature of 30°C was retained for all subsequent reactions.

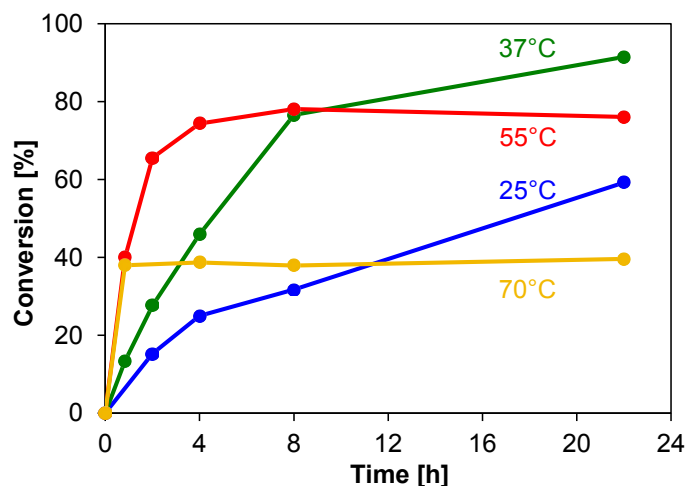


**Figure S1.** Effect of temperature and time of incubation on overall conversion of AvPAL-catalysed amination of 5 mM **1a**.

In order to intensify the reaction, the maximum possible concentrations of each of the fluorocinnamate substrates **1a-c** in the reaction buffer were ascertained (Figure S2). For **1a** the highest concentration observed before past which precipitate remained was ~200 mM, with ~150 and ~100 mM being observed for the *meta*- and *para*-isomers respectively. From these stock solutions, dilutions of 1:5, 1:10, 1:20 and 1:40 were prepared with the neat reaction buffer and 5 mg mL<sup>-1</sup> catalyst added to afford biotransformation mixtures to test substrate loading. With each substrate it was found that increased concentration of starting material had a positive effect on calculated product yield, whilst giving a nonlinear decrease in overall conversion. Interestingly **2a** was found to give greater conversions than the other two isomers at concentrations exceeding 7.5 mM, despite **1a** being the best substrate initially.

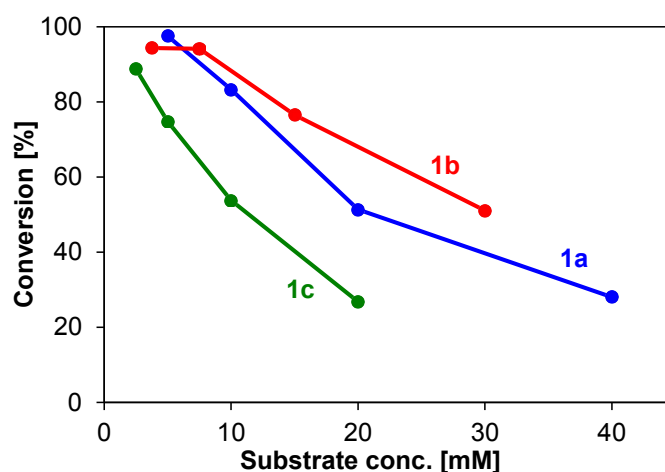


**Figure S2.** Effect of substrate loading on overall conversion of AvPAL-catalysed amination of **1a-c**.

As appropriate conversions of >95% were achieved only at low substrate concentrations, it was reasoned that the amination reactions could be improved by increased catalyst loading. This was first done via the sequential supplementation of 5 mg batches of lyophilised whole cell biocatalyst in

separate 1 mL biotransformations of maximum substrate concentration for each compound, with conversion monitored at various time points between additions (Figure S3). Although all three fluorinated substrates gave increases in overall conversion following each injection of catalyst, the *meta*- compound **1b** was found to give the most striking result (91-93% after 5 batches). This was in accordance with an equilibrium study performed as for the amination reactions but with 150 mM enantiopure product (*S*)-**2b**, which gave 8-10% conversion to **1b** – values which could not be increased, even upon two further additions of dry whole cells. Similar results (12-14% conversion to the cinnamate derivative) were found with 100 mM (*S*)-**2c**, despite corresponding conversions of 86-88% not being evident in the amination direction. Identification of the possible equilibrium point of the reaction prompted investigation of increased catalyst loading to 20 and 40 mg mL<sup>-1</sup> (Figure S4). Again **1b** was found to be consumed to the greatest extent (86% vs. <50% with 40 mg mL<sup>-1</sup> after 22 hours), but equilibrium conversions of >90% were not achieved.

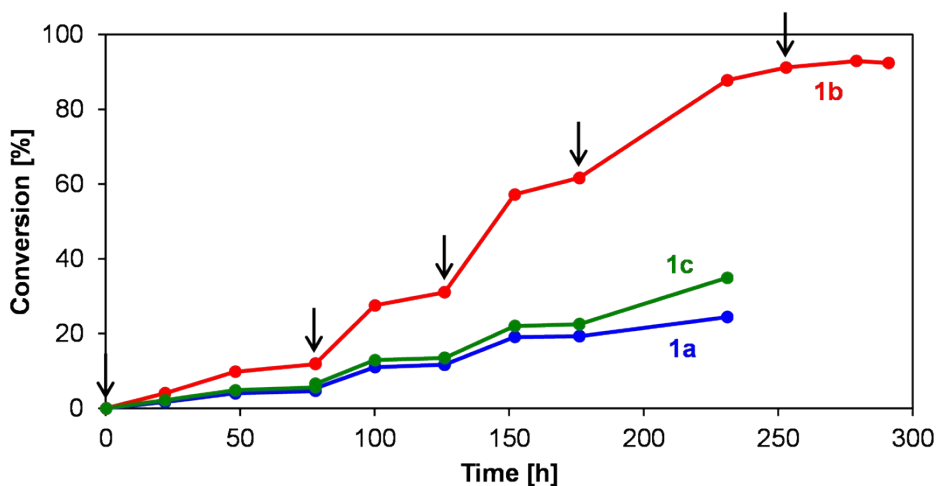


**Figure S3.** Effect of batch addition of 5 mg mL<sup>-1</sup> biocatalyst on overall conversion of AvPAL-catalysed amination of **1a-c** (each catalyst addition event is indicated by a black arrow).

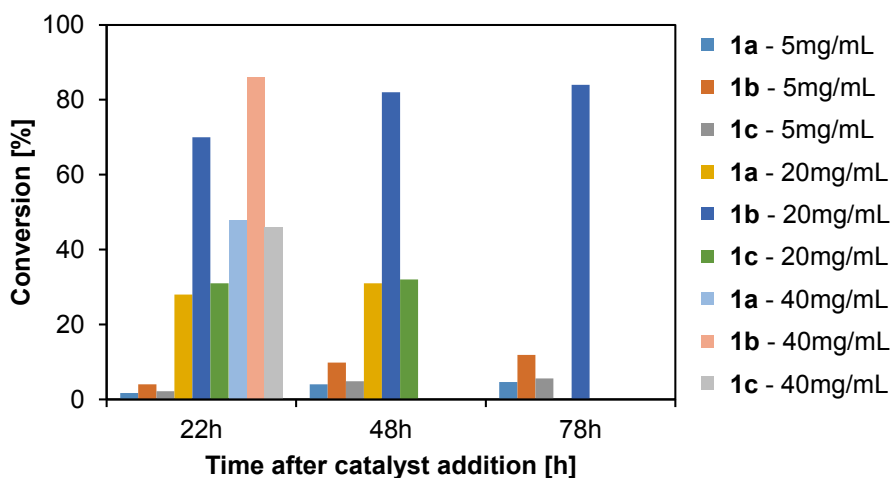


**Figure S4.** Effect of varying biocatalyst loading on overall conversion of AvPAL-catalysed amination of **1a-c**.

To test the effect of pH on the amination of the best substrate **1b**, six CO<sub>2</sub> buffered solutions of 13% NH<sub>4</sub>OH (pH 9.5-12.0) were set up and used in biotransformations with 150 mM substrate as before but using 20 mg mL<sup>-1</sup> lyophilised whole cell biocatalyst. Interestingly after 22 h at pH 9.5, a conversion of 93% was observed, compared with just 68% at pH 10.0 and 6% or less at pH 10.5 and above. Even after 8 h, the lowest pH reaction buffer was observed to give a higher conversion than the next best buffer at pH 10 after 22 h (76% vs. 68%). Unfortunately the prospect of even further improvements with solutions of pH <9.5 could not be realised using this method, due to the lower solubility of ammonium carbonate under these conditions, leading to sudden precipitation of the salt upon further buffering with CO<sub>2</sub>.

**Table S2.** Effect of varying pH on overall conversion of AvPAL-catalysed amination of **1b**.

pH	9.5	10.0	10.5	11.0	11.5	12.0
Conv. (8 h) [%]	76	36	6	5	3	4
Conv. (22 h) [%]	93	68	14	7	5	4

### Optimisation of the gram scale amination of 1b with ammonium carbamate

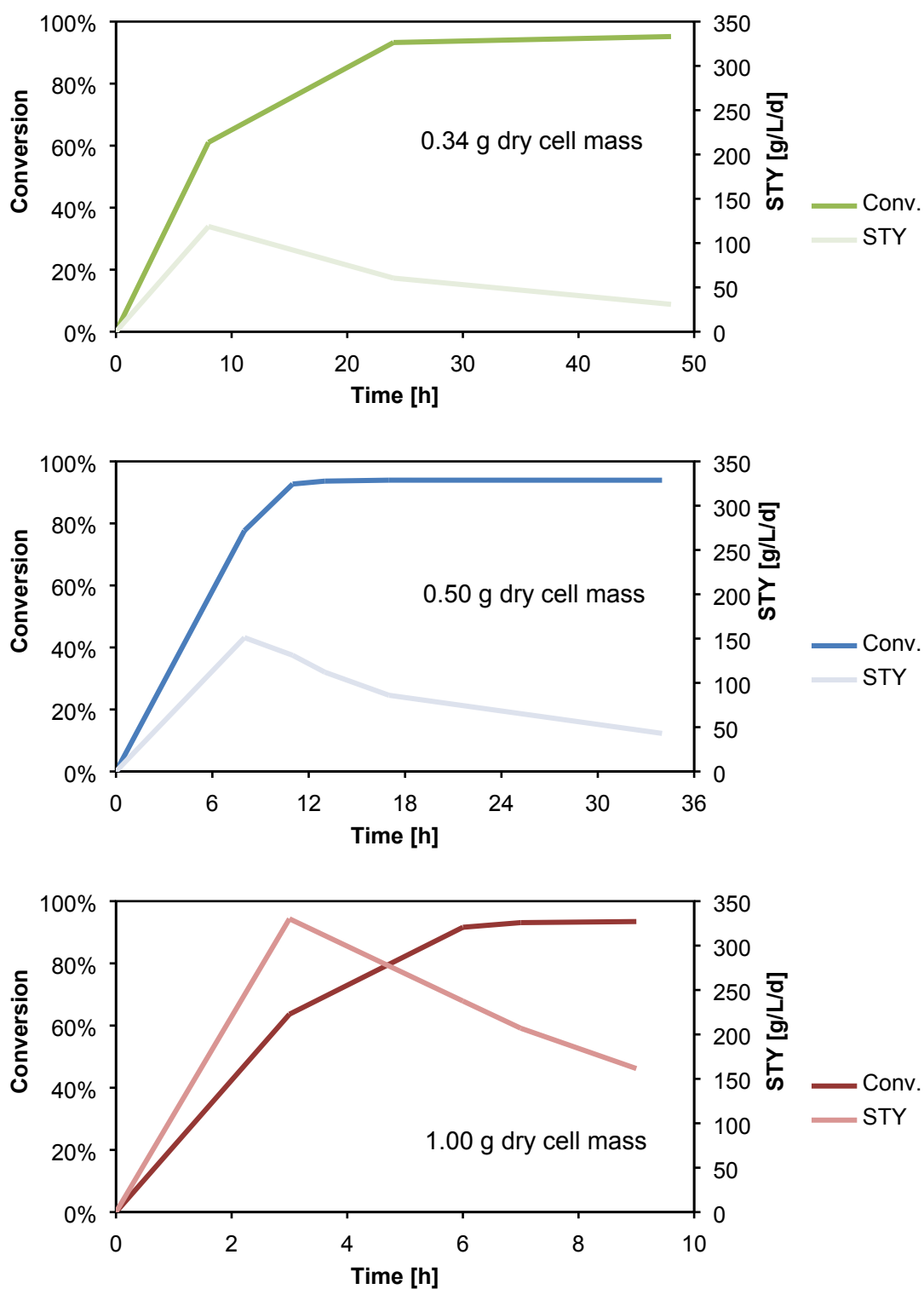


**Figure S5.** Effect of catalyst loading on overall conversion and space time yield (STY) over time for gram scale AvPAL-catalysed syntheses of (S)-2b (in 17 mL reaction volume).

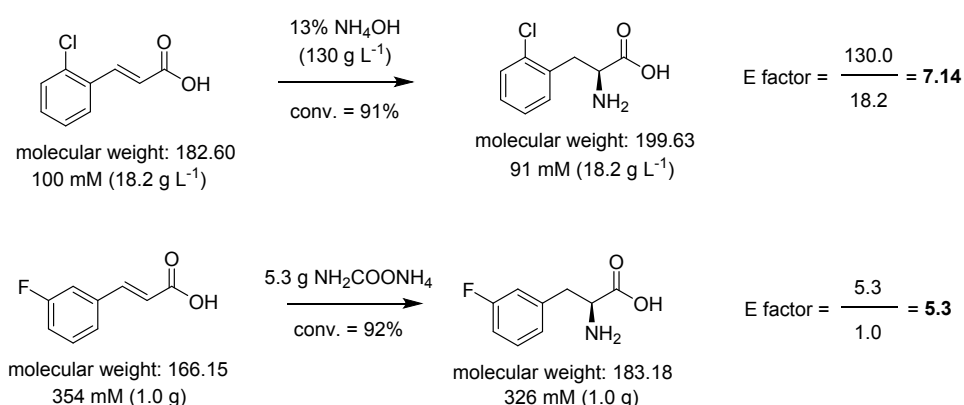
HPLC analyses at various time points revealed an increase in reaction rate and initial space time yield (STY) values with increasing biocatalyst mass. All reactions were observed to reach equilibrium conversions of 93-95% after varying amounts of time. Although the largest STY (330.2 g L<sup>-1</sup> d<sup>-1</sup>) was seen after a 3 h reaction time with 1.0 g biocatalyst, the conversion of only 64% was not deemed amenable for further crude isolation steps. For this reason a reaction time of 6 h with 1.0 g biocatalyst was chosen as an optimised method, balancing high conversion (92%) with a still impressive STY of 237.6 g L<sup>-1</sup> d<sup>-1</sup>).

### Calculation of E factor values

E factors<sup>S4</sup> were calculated using only chemical species that participate in the reaction (i.e. not catalyst or chemicals for pH adjustment). Water was discounted or included depending on the calculation required.

For the reported DSM method the values for total starting material (18.2 g L<sup>-1</sup> cinnamate and 130 g L<sup>-1</sup> ammonia) and product (18.2 g L<sup>-1</sup> amino acid) are used as stated in the publication where they are reported. An estimate of the E factor including water was calculated using a figure for water mass, calculated by subtracting the mass of the starting materials from the overall mass of the 1 L reaction vessel (~1000 g – 148.2 g = ~851.8 g).

For the gram-scale synthesis of (S)-**2b** the product value (1.0 g) was calculated using the conversion (92%) multiplied by the concentration of the cinnamate starting material (354 mM) to give a product concentration, which was then converted to a mass per 17 mL reaction. The E factor including water was calculated by adding the 17 g water used to the waste mass.



## HPLC analysis and representative traces

Reverse phase HPLC was performed on an Agilent 1200 Series LC system equipped with a G1379A degasser, a G1312A binary pump, a G1329 autosampler unit, a G1316A temperature controlled column compartment and a G1315B diode array detector.

### Conversion

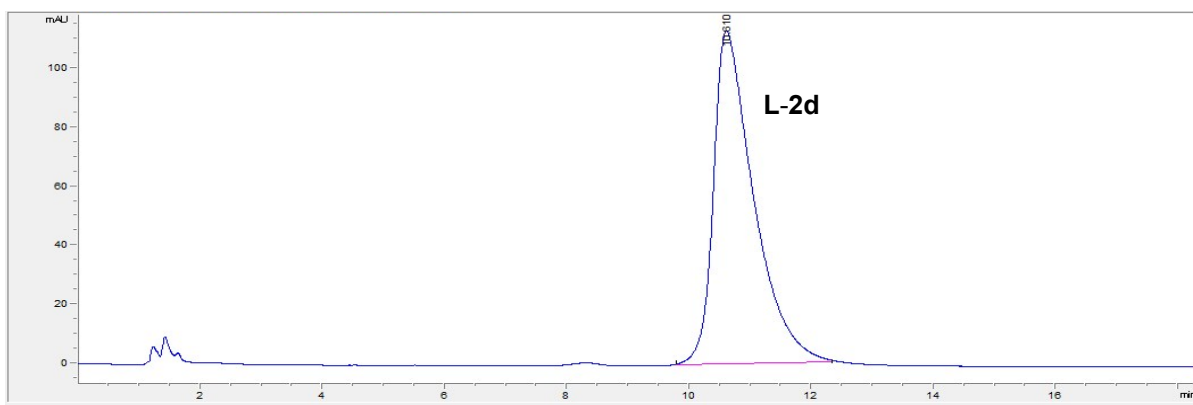
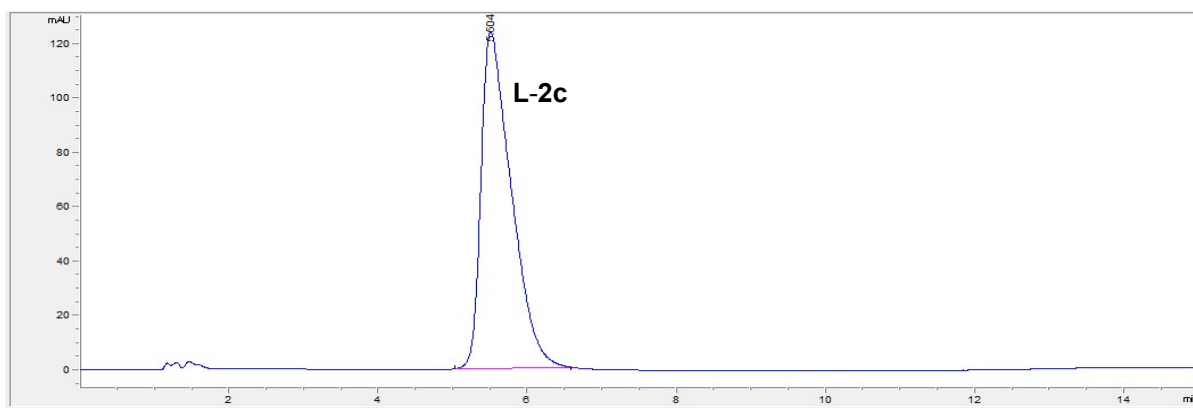
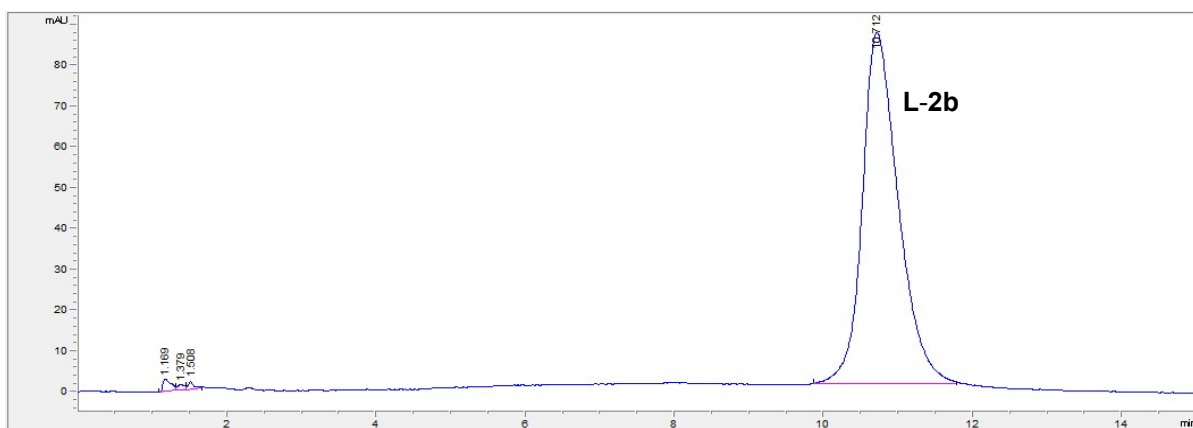
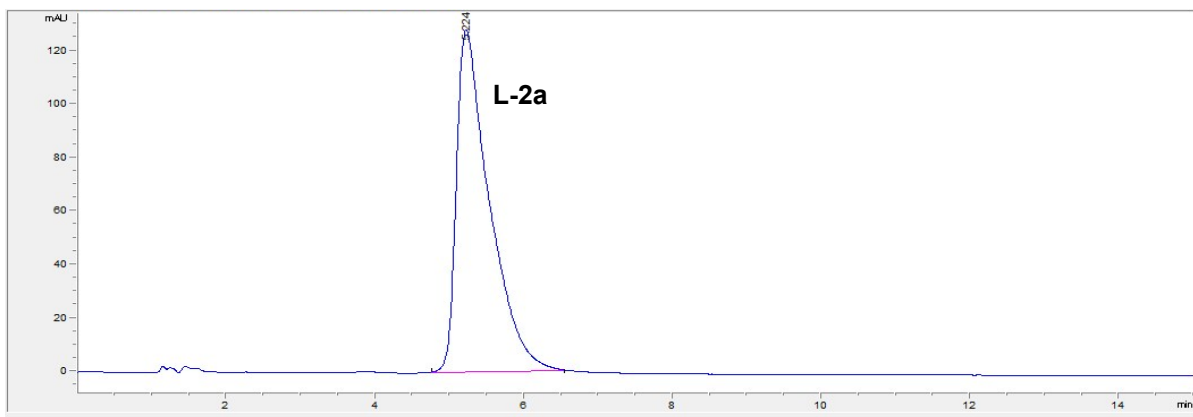
Reaction conversions for the PAL biotransformations were measured by reverse phase HPLC on a non-chiral Zorbax C-18 Extend column (50 mm × 4.6 mm × 3.5 μm, Agilent), flow rate 1.0 mL min<sup>-1</sup>, temperature 40°C, detection wavelength 210 nm. Method 1 (mobile phase: aq. NH<sub>4</sub>OH 0.1 M pH 10 / MeOH, 9:1). Method 2 (mobile phase: aq. NH<sub>4</sub>OH 0.1 M pH 10 / MeOH, 8:2). Method 3 (mobile phase: aq. NH<sub>4</sub>OH 0.1 M pH 10 / MeOH, 7:3). Method 4 (mobile phase: aq. NH<sub>4</sub>OH 0.1 M pH 10 / MeOH, 6:4). Retention times are reported in the following table.

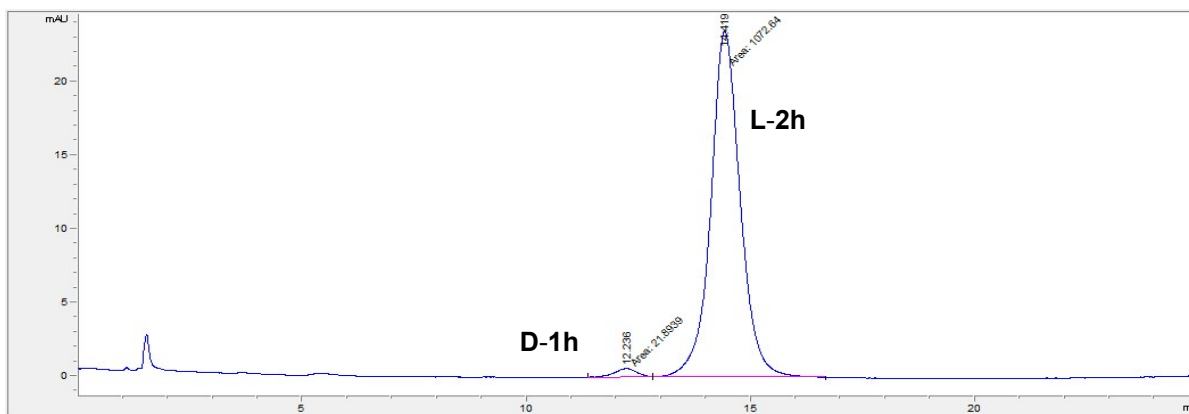
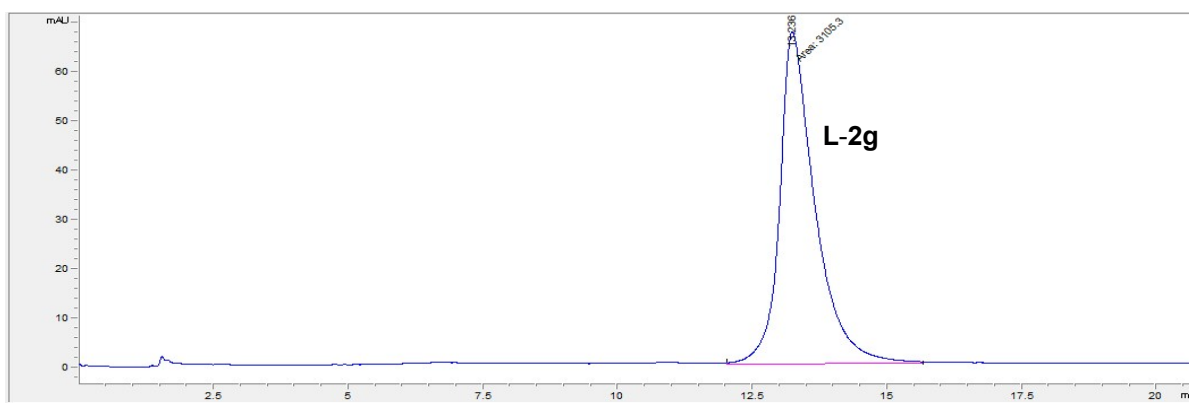
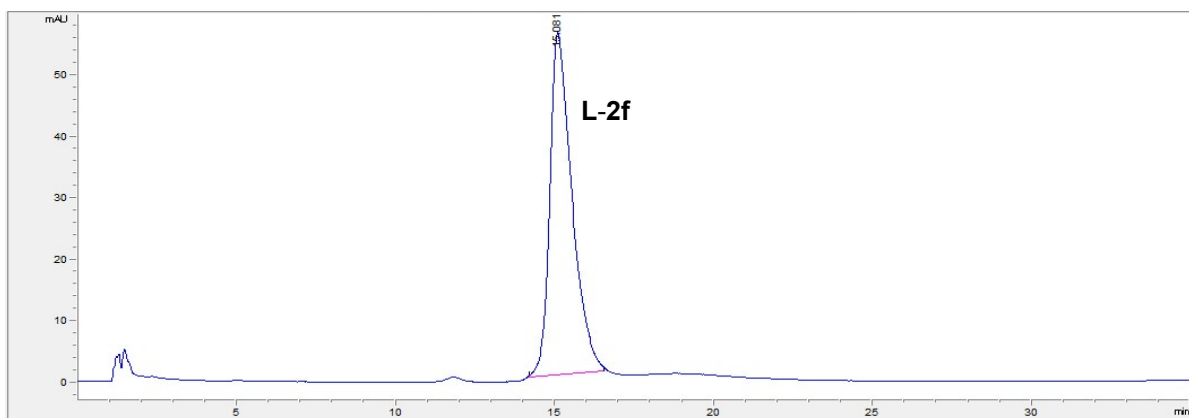
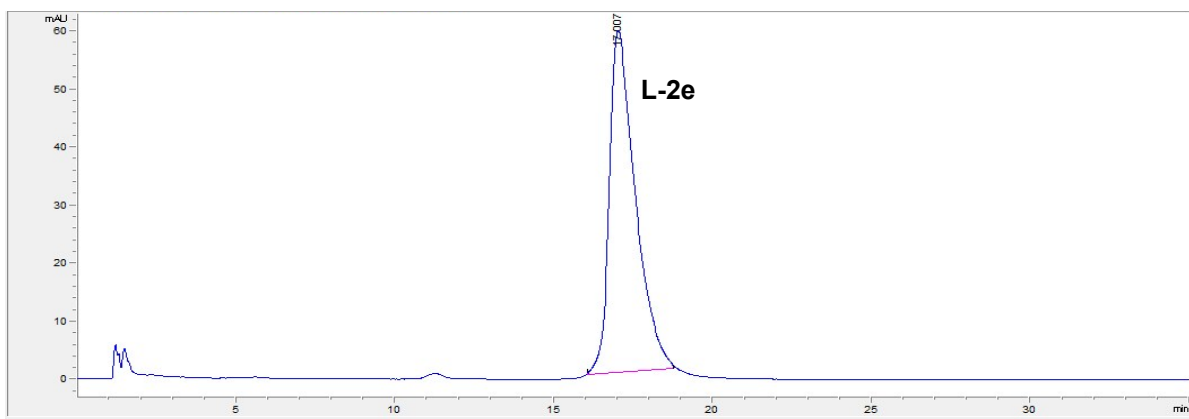
Compound	<i>t<sub>R</sub></i> (min)	Method	Compound	<i>t<sub>R</sub></i> (min)	Method
<b>1a</b>	4.5	1	<b>2a</b>	1.7	1
<b>1b</b>	4.1	1	<b>2b</b>	1.6	1
<b>1c</b>	3.7	1	<b>2c</b>	1.6	1
<b>1d</b>	4.9	2	<b>2d</b>	2.0	2
<b>1e</b>	3.8	3	<b>2e</b>	1.6	3
<b>1f</b>	6.9	3	<b>2f</b>	2.9	3
<b>1g</b>	5.0	3	<b>2g</b>	2.1	3
<b>1h</b>	7.0	3	<b>2h</b>	2.9	3
<b>1i</b>	5.1	4	<b>2i</b>	2.1	4
<b>1j</b>	6.8	3	<b>2j</b>	2.6	3

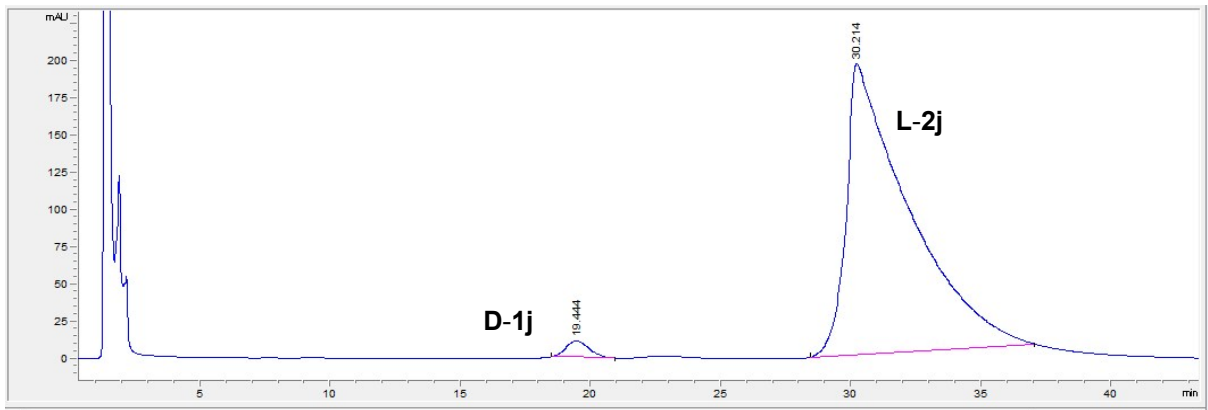
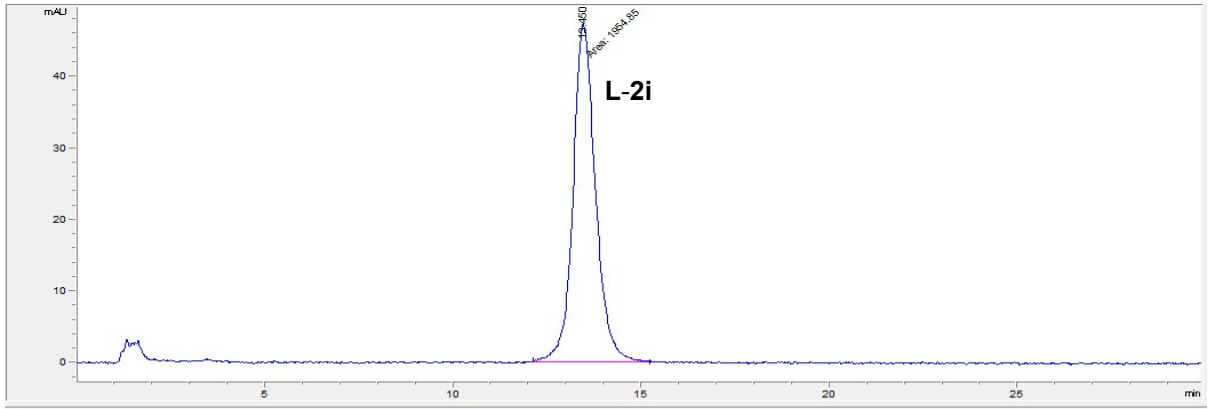
### Enantiomeric excess

Enantiomeric excess of product **2a-j** were determined by reverse phase HPLC on a chiral CROWNPAK CR(+) column (150 mm × 4 mm × 5 μm, Daicel), flow rate 1.0 mL min<sup>-1</sup>, detection wavelength 210 nm, mobile phase: aq. HClO<sub>4</sub> 1.14% pH 2 / MeOH, 96:4. Retention times are reported in the following table and representative HPLC traces are shown below.

Compound	<i>t<sub>R</sub></i> (min)
<b>(S)-2a</b>	5.2
<b>(S)-2b</b>	10.7
<b>(S)-2c</b>	5.5
<b>(S)-2d</b>	10.6
<b>(S)-2e</b>	17.0
<b>(S)-2f</b>	15.1
<b>(S)-2g</b>	13.2
<b>(S)-2h</b>	14.4
<b>(S)-2i</b>	13.4
<b>(S)-2j</b>	30.2

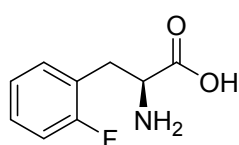






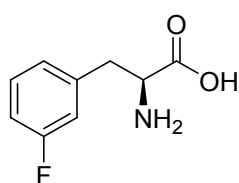
## Characterisation data of compounds 1a-j and 4

### (S)-2-amino-3-(2-fluorophenyl)propanoic acid (1a)



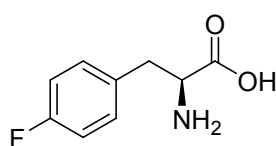
White solid (181 mg) **<sup>1</sup>H NMR** (400 MHz, D<sub>2</sub>O+NaOH) 7.16-7.22 (2H, m), 6.99-7.07 (2H, m), 3.38-3.42 (1H, m), 2.88-2.93 (1H, dd, *J* = 16 Hz, 8 Hz), 2.74-2.80 (1H, dd, *J* = 16 Hz, 8 Hz) **<sup>13</sup>C NMR** (100 MHz, D<sub>2</sub>O+NaOH) 182.17, 161.21 (d, <sup>1</sup>*J*<sub>CF</sub> = 242 Hz), 131.73 (d, <sup>3</sup>*J*<sub>CF</sub> = 5 Hz), 128.55 (d, <sup>3</sup>*J*<sub>CF</sub> = 8 Hz), 125.02 (d, <sup>2</sup>*J*<sub>CF</sub> = 16 Hz), 124.23 (d, <sup>4</sup>*J*<sub>CF</sub> = 4 Hz), 115.19 (d, <sup>2</sup>*J*<sub>CF</sub> = 22 Hz), 57.69, 34.21 **HRMS** (ESI, *m/z*) calcd. mass 184.0774 [M+H]<sup>+</sup>, found 184.0702 [M+H]<sup>+</sup>.

### (S)-2-amino-3-(3-fluorophenyl)propanoic acid (1b)



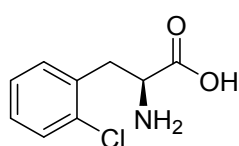
White solid (180 mg) **<sup>1</sup>H NMR** (400 MHz, D<sub>2</sub>O+NaOH) 7.20-7.26 (1H, m), 6.89-6.96 (3H, m), 3.38 (1H, m), 2.84-2.89 (1H, dd, *J* = 16 Hz, 12 Hz), 2.71-2.76 (1H, dd, *J* = 16 Hz, 12 Hz) **<sup>13</sup>C NMR** (100 MHz, D<sub>2</sub>O+NaOH) 182.17, 162.56 (d, <sup>1</sup>*J*<sub>CF</sub> = 242 Hz), 140.85 (d, <sup>3</sup>*J*<sub>CF</sub> = 8 Hz), 130.06 (d, <sup>3</sup>*J*<sub>CF</sub> = 8 Hz), 125.19 (d, <sup>4</sup>*J*<sub>CF</sub> = 2 Hz), 115.91 (d, <sup>2</sup>*J*<sub>CF</sub> = 21 Hz), 113.25 (d, <sup>2</sup>*J*<sub>CF</sub> = 21 Hz), 57.32, 40.49 **HRMS** (ESI, *m/z*) calcd. mass 184.0774 [M+H]<sup>+</sup>, found 184.0693 [M+H]<sup>+</sup>.

### (S)-2-amino-3-(4-fluorophenyl) propanoic acid (1c)



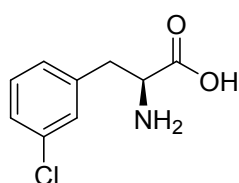
White solid (175 mg) **<sup>1</sup>H NMR** (400 MHz, D<sub>2</sub>O+NaOH) 7.11-7.14 (2H, m), 6.94-6.99 (2H, m), 3.34-3.37 (1H, m), 2.80-2.85 (1H, dd, *J* = 16 Hz, 8 Hz), 2.70-2.75 (1H, dd, *J* = 16 Hz, 8 Hz) **<sup>13</sup>C NMR** (100 MHz, D<sub>2</sub>O+NaOH) 182.34, 161.48 (d, <sup>1</sup>*J*<sub>CF</sub> = 240 Hz), 133.95 (d, <sup>4</sup>*J*<sub>CF</sub> = 3 Hz), 130.87 (d, <sup>3</sup>*J*<sub>CF</sub> = 8 Hz), 115.04 (d, <sup>2</sup>*J*<sub>CF</sub> = 21 Hz), 57.45, 39.89 **HRMS** (ESI, *m/z*) calcd. mass 184.0774 [M+H]<sup>+</sup>, found 184.0677 [M+H]<sup>+</sup>.

### (S)-2-amino-3-(2-chlorophenyl)propanoic acid (1d)



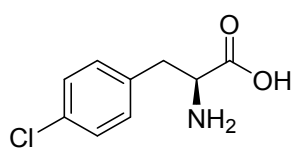
Pale yellow solid (90 mg) **<sup>1</sup>H NMR** (400 MHz, D<sub>2</sub>O+NaOH) 7.31-7.33 (1H, m), 7.12-7.20 (3H, m), 3.43-3.46 (1H, m), 2.96-3.01 (1H, dd, *J* = 12 Hz, 8 Hz), 2.79-2.84 (1H, dd, *J* = 12 Hz, 8 Hz) **<sup>13</sup>C NMR** (100 MHz, D<sub>2</sub>O+NaOH) 182.35, 135.99, 133.83, 131.62, 129.39, 128.22, 127.03, 56.51, 38.63 **HRMS** (ESI, *m/z*) calcd. mass 200.0478 [M+H]<sup>+</sup>, found 200.0400 [M+H]<sup>+</sup>.

### (S)-2-amino-3-(3-chlorophenyl) propanoic acid (1e)



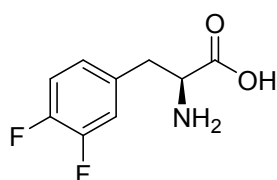
Pale yellow solid (87 mg) **<sup>1</sup>H NMR** (400 MHz, D<sub>2</sub>O+NaOH) 1.17-7.20 (3H, m), 7.06 (1H, d, *J* = 8 Hz), 3.35-3.38 (1H, m), 2.82-2.86 (1H, dd, *J* = 12 Hz, 4 Hz), 2.68-2.73 (1H, dd, *J* = 12 Hz, 8 Hz) **<sup>13</sup>C NMR** (100 MHz, D<sub>2</sub>O+NaOH) 182.09, 140.42, 133.45, 129.91, 129.13, 127.72, 126.53, 57.32, 40.42 **HRMS** (ESI, *m/z*) calcd. mass 200.0478 [M+H]<sup>+</sup>, found 200.0383 [M+H]<sup>+</sup>.

**(S)-2-amino-3-(4-chlorophenyl) propanoic acid (1f)**



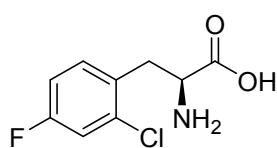
Pale yellow solid (86 mg)  $^1\text{H NMR}$  (400 MHz,  $\text{D}_2\text{O}+\text{NaOH}$ ) 7.23 (2H, d,  $J = 8$  Hz), 7.10 (2H, d,  $J = 8$  Hz), 3.34-3.37 (1H, m), 2.80-2.84 (1H, dd,  $J = 12$  Hz, 4 Hz), 2.68-2.73 (1H, dd,  $J = 12$  Hz, 4 Hz)  $^{13}\text{C NMR}$  (100 MHz,  $\text{D}_2\text{O}+\text{NaOH}$ ) 182.20, 136.85, 131.64, 130.83, 128.34, 57.33, 40.09 **HRMS** (ESI,  $m/z$ ) calcd. mass 200.0478  $[\text{M}+\text{H}]^+$ , found 200.0369  $[\text{M}+\text{H}]^+$ .

**(S)-2-amino-3-(3, 4-difluorophenyl) propanoic acid (1g)**



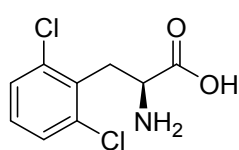
White solid (195 mg)  $^1\text{H NMR}$  (400 MHz,  $\text{D}_2\text{O}+\text{NaOH}$ ) 6.99-7.22 (2H, m), 6.88-6.91 (1H, m), 3.34-3.38 (1H, m), 2.79-2.84 (1H, dd,  $J = 16$  Hz, 8 Hz), 2.68-2.74 (1H, dd,  $J = 16$  Hz, 8 Hz)  $^{13}\text{C NMR}$  (100 MHz,  $\text{D}_2\text{O}+\text{NaOH}$ ) 182.03, 149.68 (dd,  $^1J_{\text{CF}} = 243$  Hz,  $^2J_{\text{CF}} = 12$  Hz), 148.77 (dd,  $^1J_{\text{CF}} = 241$  Hz,  $^2J_{\text{CF}} = 12$  Hz), 135.35 (dd,  $^3J_{\text{CF}} = 5$  Hz,  $^4J_{\text{CF}} = 3$  Hz), 125.52 (dd,  $^3J_{\text{CF}} = 6$  Hz,  $^4J_{\text{CF}} = 3$  Hz), 117.83 ( $^2J_{\text{CF}} = 17$  Hz), 116.98 ( $^2J_{\text{CF}} = 17$  Hz), 57.35, 39.95 **HRMS** (ESI,  $m/z$ ) calcd. mass 202.0680  $[\text{M}+\text{H}]^+$ , found 202.0611  $[\text{M}+\text{H}]^+$ .

**(S)-2-amino-3-(2-chloro-4-fluorophenyl) propanoic acid (1h)**



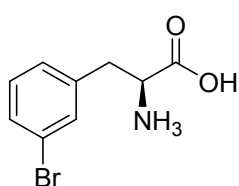
White solid (208 mg)  $^1\text{H NMR}$  (400 MHz,  $\text{D}_2\text{O}+\text{NaOH}$ ) 7.12-7.20 (2H, m), 6.91-6.96 (1H, m), 3.41-3.44 (1H, m), 2.93-2.98 (1H, dd,  $J = 16$  Hz, 8 Hz), 2.77-2.82 (1H, dd,  $J = 12$  Hz, 8 Hz)  $^{13}\text{C NMR}$  (100 MHz,  $\text{D}_2\text{O}+\text{NaOH}$ ) 182.21, 161.09 (d,  $^1J_{\text{CF}} = 244$  Hz), 134.28 (d,  $^3J_{\text{CF}} = 10$  Hz), 132.46 (d,  $^3J_{\text{CF}} = 8$  Hz), 132.01 (d,  $^4J_{\text{CF}} = 3$  Hz), 116.42 (d,  $^2J_{\text{CF}} = 25$  Hz), 113.99 (d,  $^2J_{\text{CF}} = 21$  Hz), 56.51, 37.92 **HRMS** (ESI,  $m/z$ ) calcd. mass 218.0384  $[\text{M}+\text{H}]^+$ , found 218.0368  $[\text{M}+\text{H}]^+$ .

**(S)-2-amino-3-(2, 6-dichlorophenyl) propanoic acid (1i)**



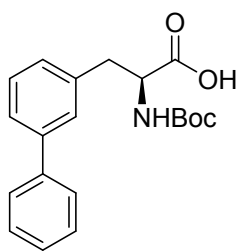
White solid (112 mg)  $^1\text{H NMR}$  (400 MHz,  $\text{D}_2\text{O}+\text{NaOH}$ ) 7.27 (2H, d,  $J = 8$  Hz), 7.08 (1H, t,  $J = 8$  Hz), 3.48-3.52 (1H, m), 3.12-3.18 (1H, dd,  $J = 16$  Hz, 8 Hz), 2.98-3.04 (1H, dd,  $J = 16$  Hz, 8 Hz)  $^{13}\text{C NMR}$  (100 MHz,  $\text{D}_2\text{O}+\text{NaOH}$ ) 182.38, 135.52, 134.32, 128.50, 128.28, 55.56, 36.17 **HRMS** (ESI,  $m/z$ ) calcd. mass 234.0089  $[\text{M}+\text{H}]^+$ , found 234.0031  $[\text{M}+\text{H}]^+$ .

**(S)-2-amino-3-(3-bromophenyl) propanoic acid (1j)**



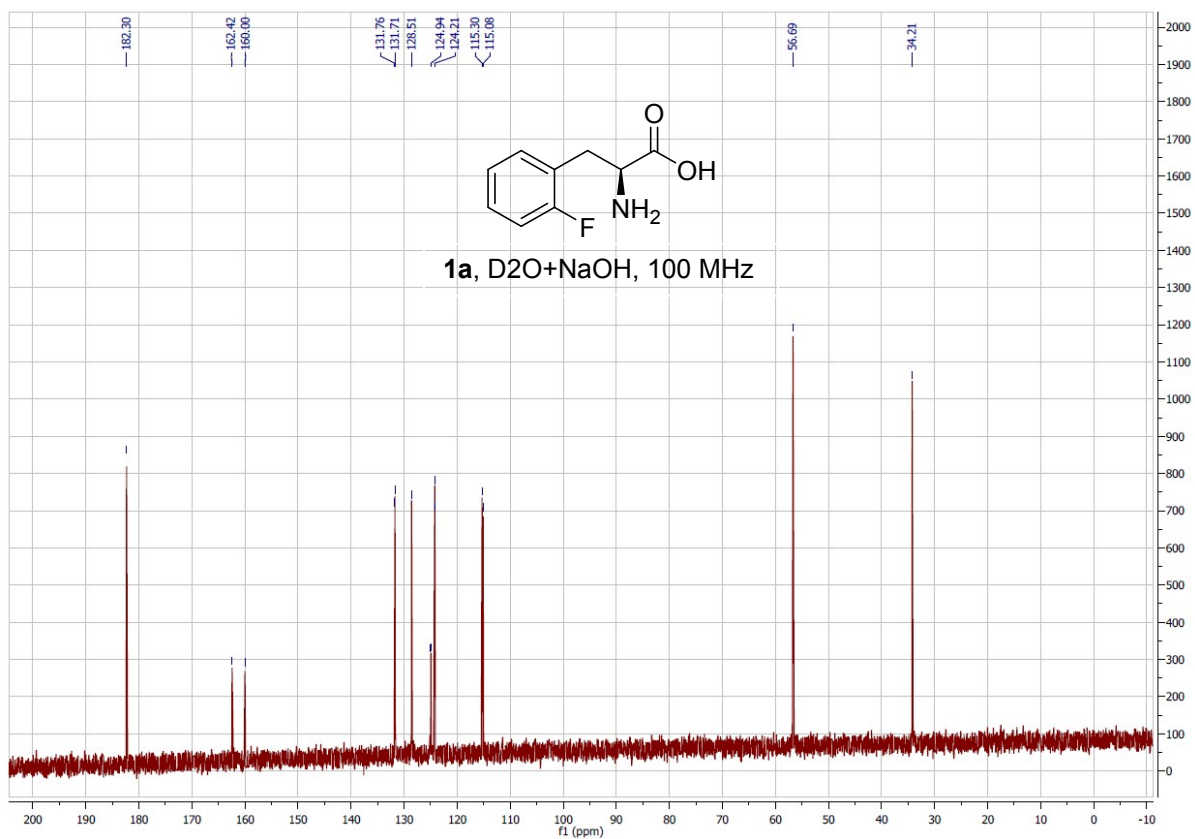
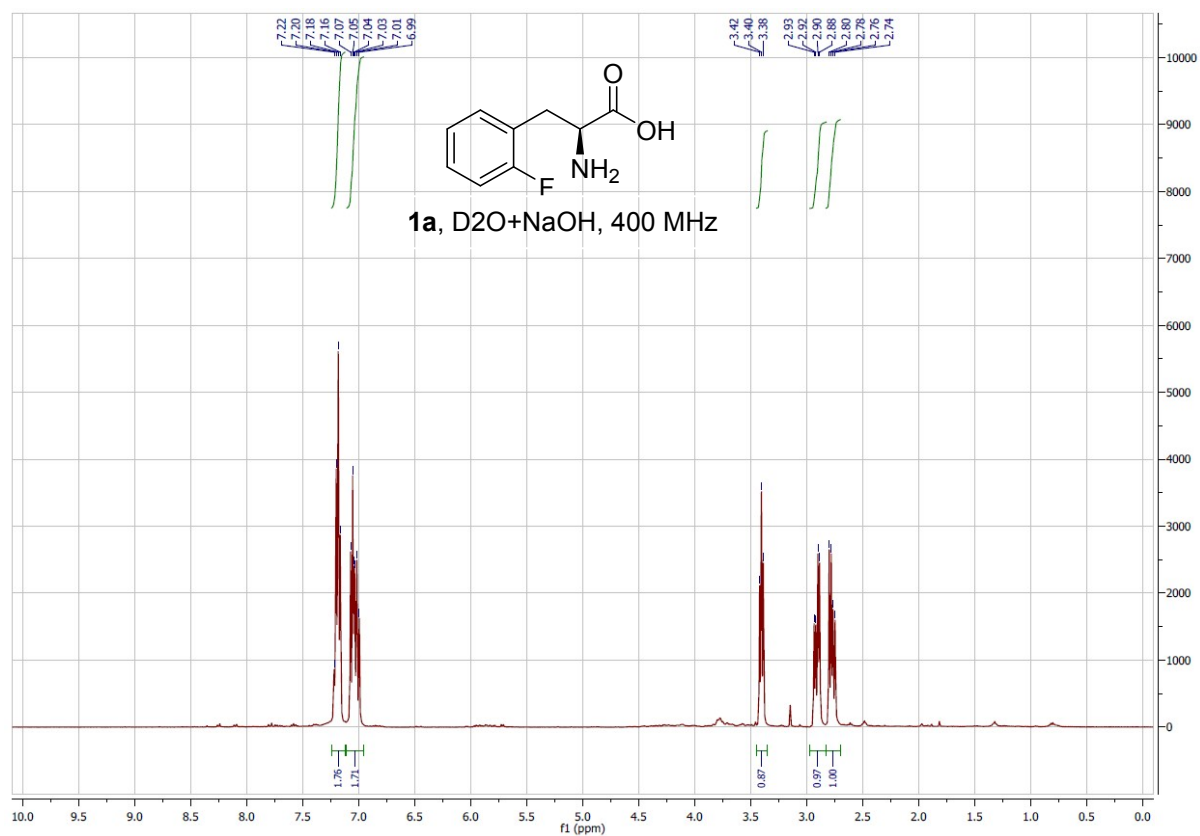
Yellowish solid (58 mg)  $^1\text{H NMR}$  (400 MHz,  $\text{D}_2\text{O}+\text{NaOH}$ ) 7.35 (2H, m), 7.10-7.17 (2H, m), 3.35-3.38 (1H, m), 2.82-2.87 (1H, dd,  $J = 9$  Hz, 4 Hz), 2.67-2.72 (1H, dd,  $J = 9$  Hz, 4 Hz)  $^{13}\text{C NMR}$  (100 MHz,  $\text{D}_2\text{O}+\text{NaOH}$ ) 182.06, 140.76, 132.06, 130.22, 129.49, 128.18, 121.77, 57.35, 40.41 **HRMS** (ESI,  $m/z$ ) calcd. mass 243.9973  $[\text{M}+\text{H}]^+$ , found 243.9845  $[\text{M}+\text{H}]^+$ .

**(S)-3-([1,1'-biphenyl]-3-yl)-2-((tert-butoxycarbonyl)amino)propanoic acid (4)**



White solid (30 mg) **<sup>1</sup>H NMR** (400 MHz, MeOH-*d*<sub>4</sub>) 7.23-7.39 (9H, m), 4.34-4.37 (1H, dd, *J* = 8 Hz, 4 Hz), 3.19-3.24 (1H, dd, *J* = 16 Hz, 4 Hz), 2.92-2.98 (1H, dd, *J* = 9 Hz, 8 Hz) **<sup>13</sup>C NMR** (100 MHz, MeOH-*d*<sub>4</sub>) 177.04, 157.73, 142.50, 139.47, 134.80, 129.82, 129.45, 129.32, 128.58, 128.33, 128.14, 126.33, 80.52, 56.97, 39.07, 28.78 **HRMS** (ESI, *m/z*) calcd. mass 364.1525 [M+Na]<sup>+</sup>, found 364.1386 [M+Na]<sup>+</sup>.

# NMR and HRMS spectra of compounds 1a-j and 4

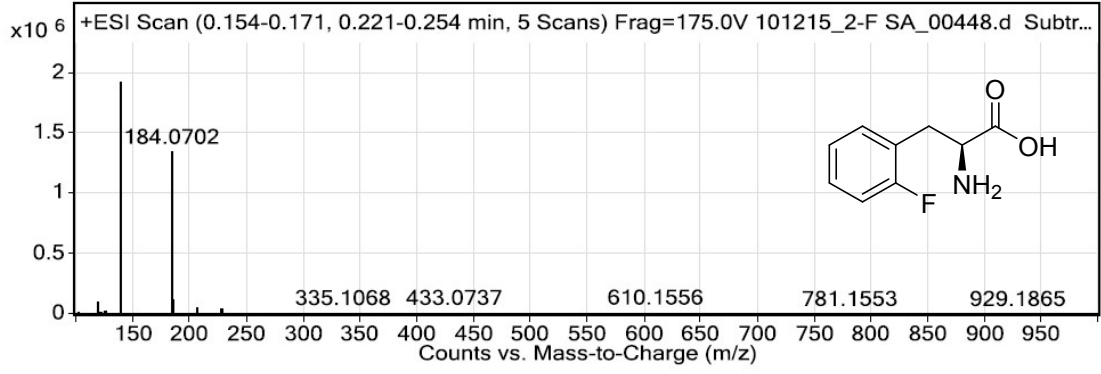


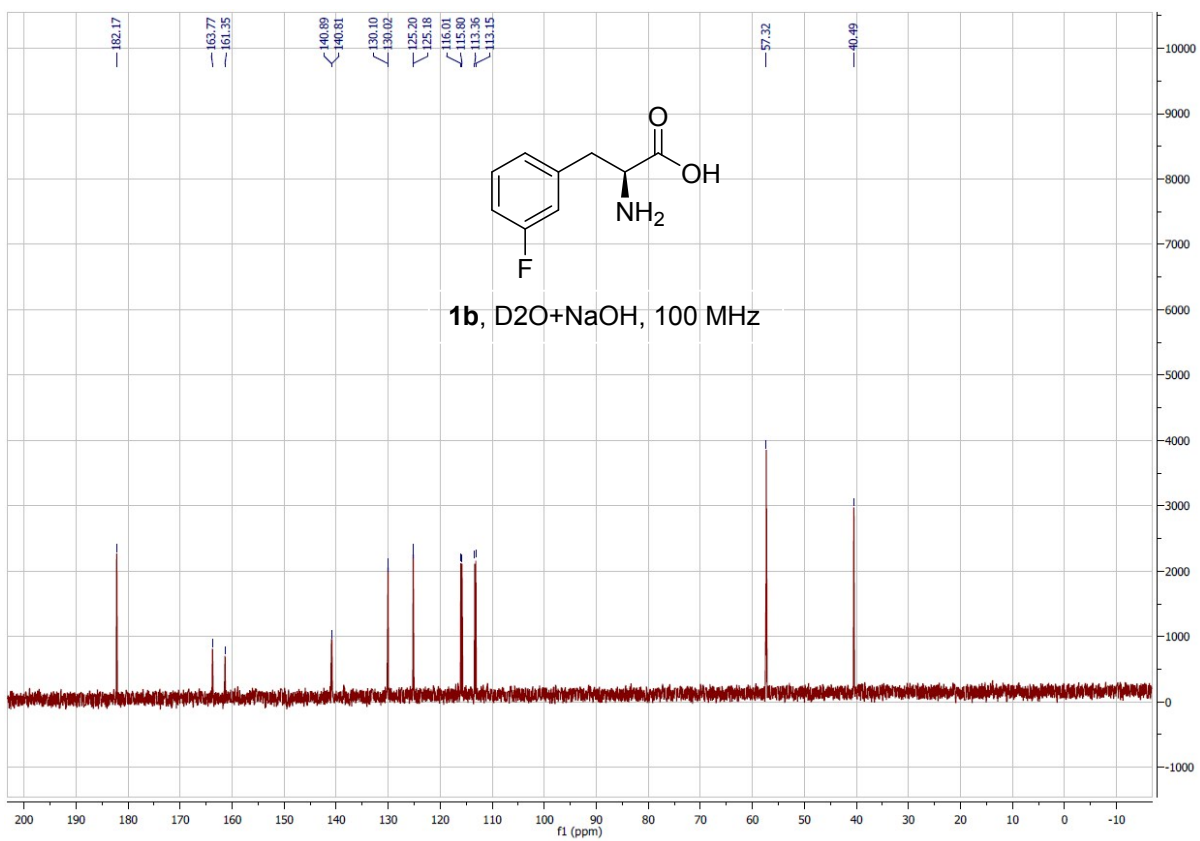
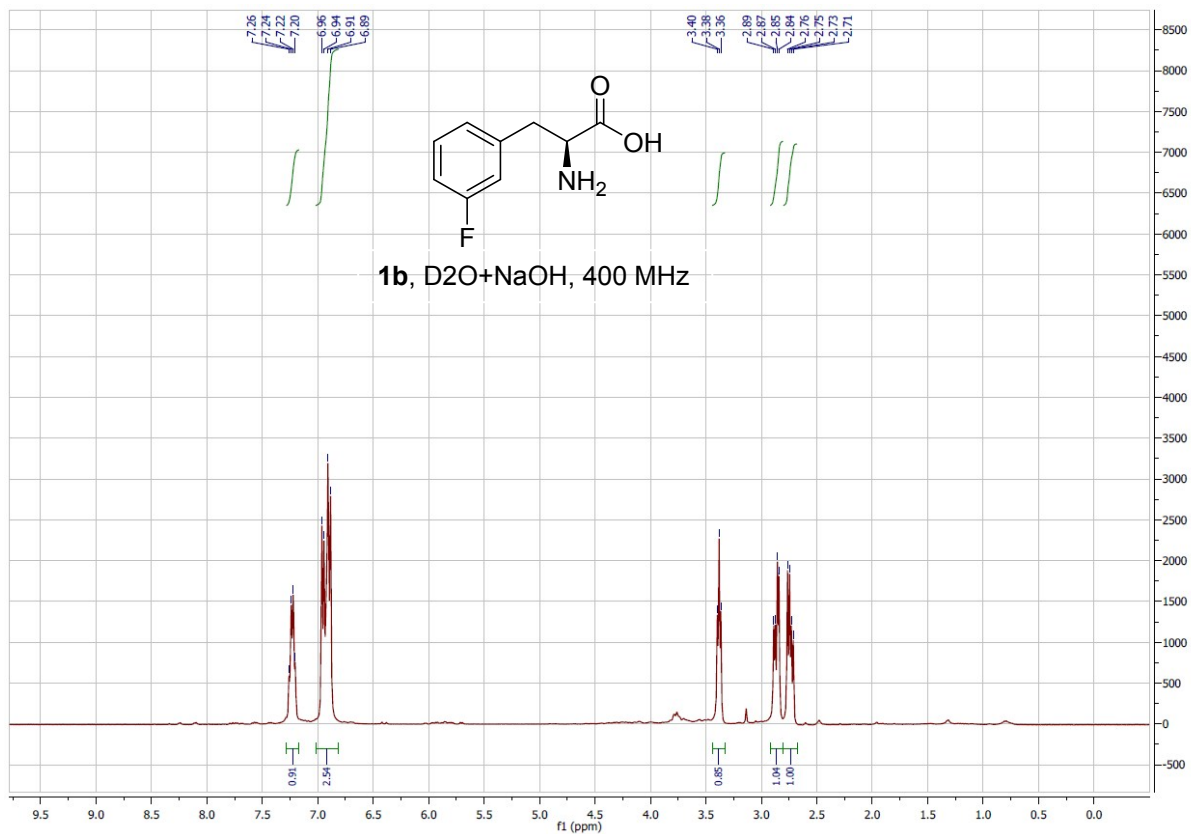
Spectrum Source  
Peak (1) in <sup>+</sup>TIC Scan Smo<sup>+</sup>

Fragmentor Voltage  
175

Collision Energy  
0

Ionization Mode  
ESI



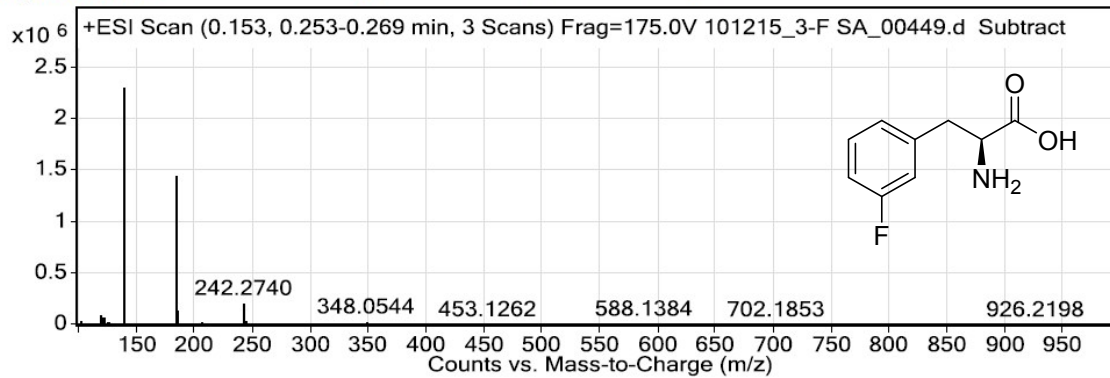


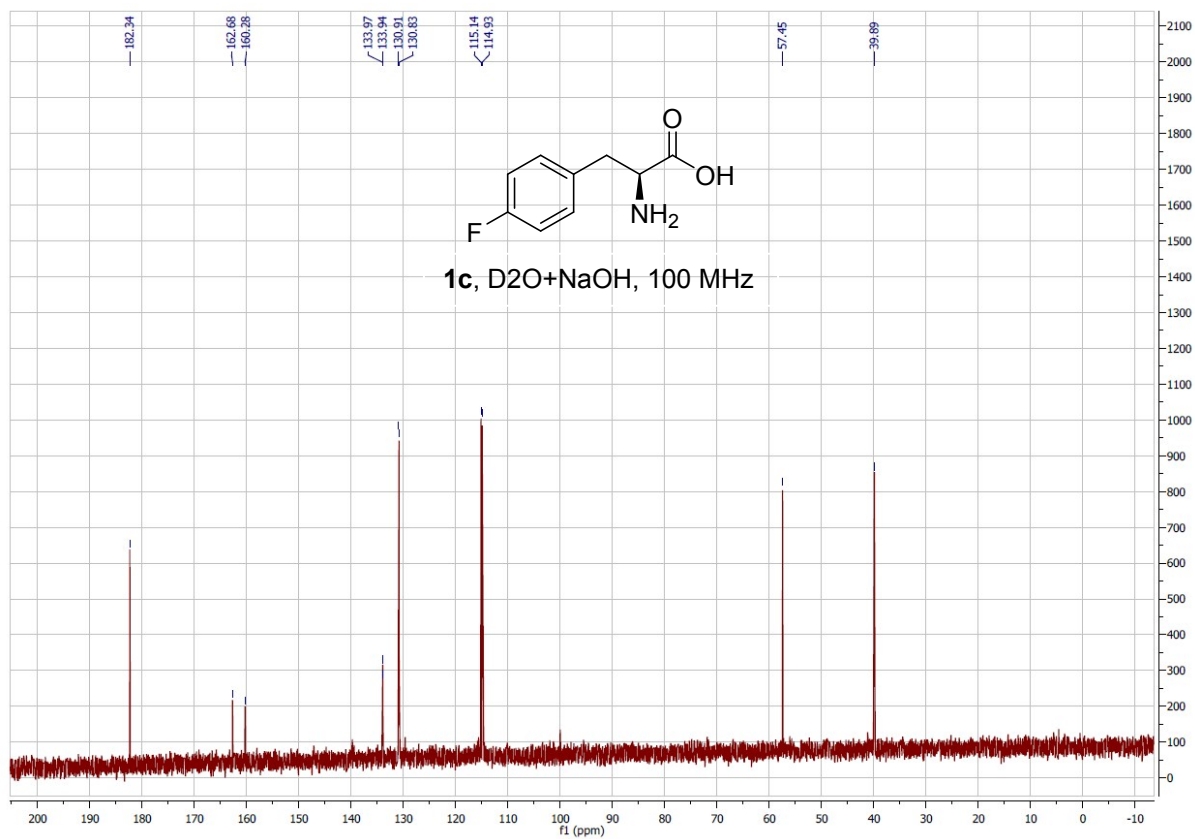
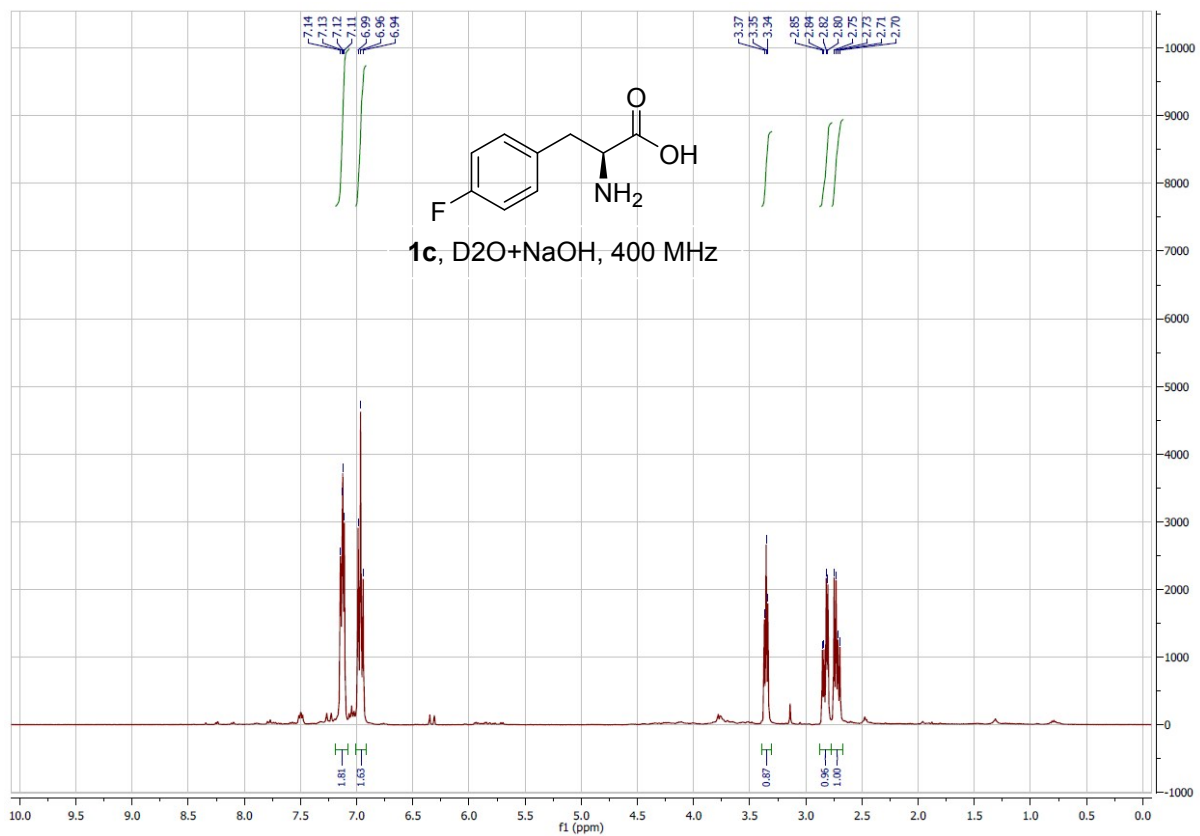
Spectrum Source  
Peak (1) in <sup>+</sup>TIC Scan Smo<sup>\*</sup>

Fragmentor Voltage  
175

Collision Energy  
0

Ionization Mode  
ESI



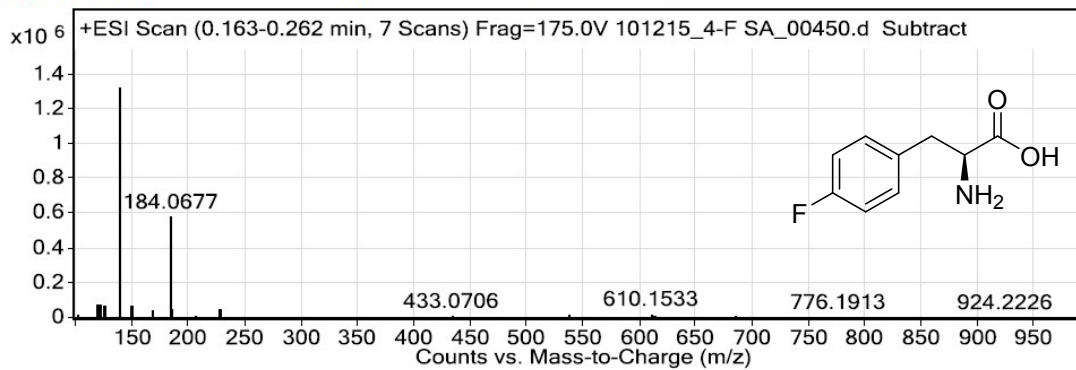


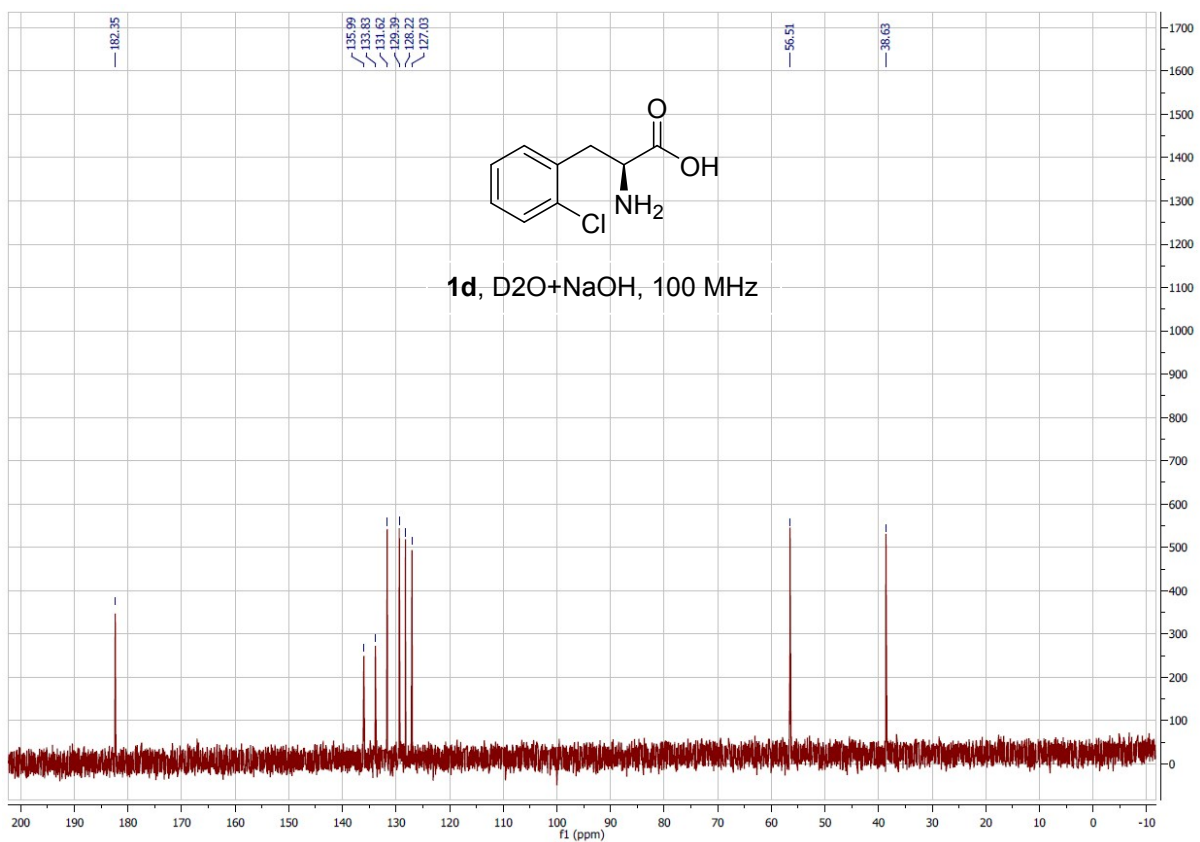
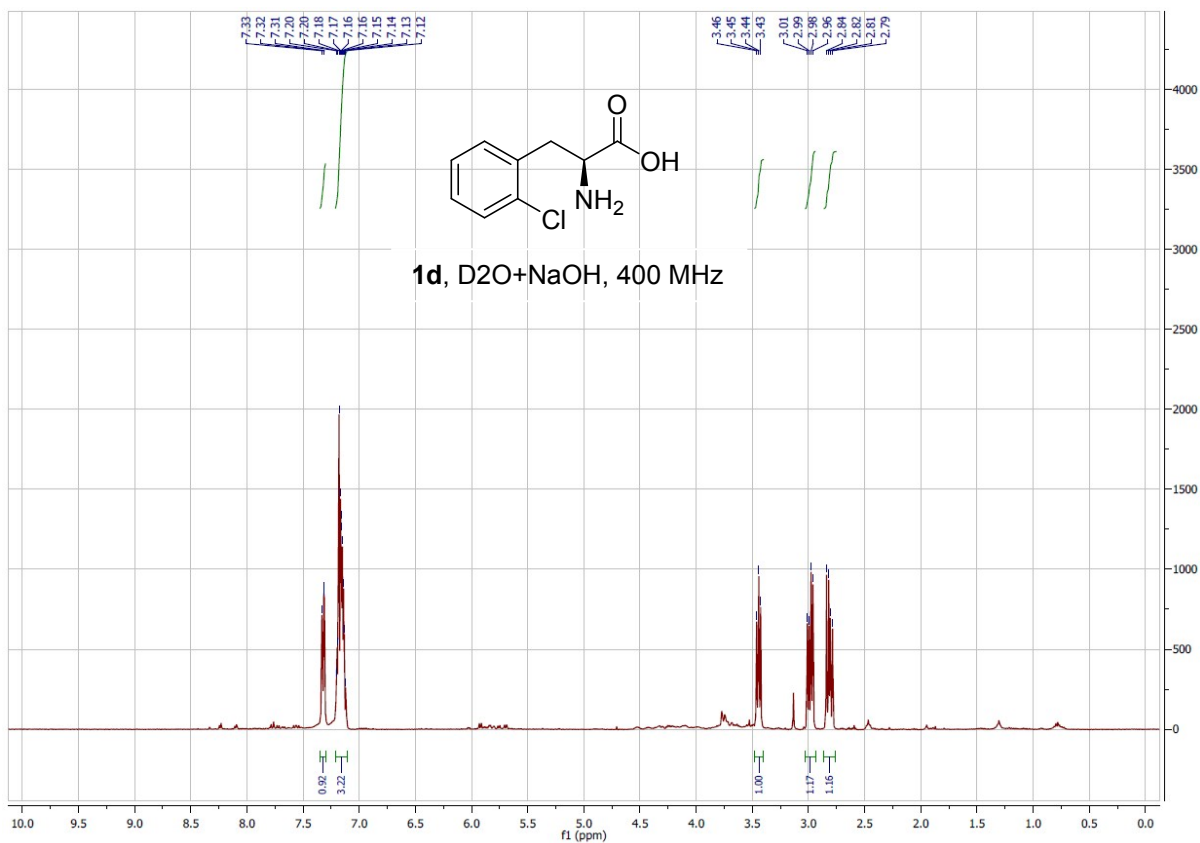
Spectrum Source  
Peak (1) in \*+ TIC Scan Smo\*

Fragmentor Voltage  
175

Collision Energy  
0

Ionization Mode  
ESI



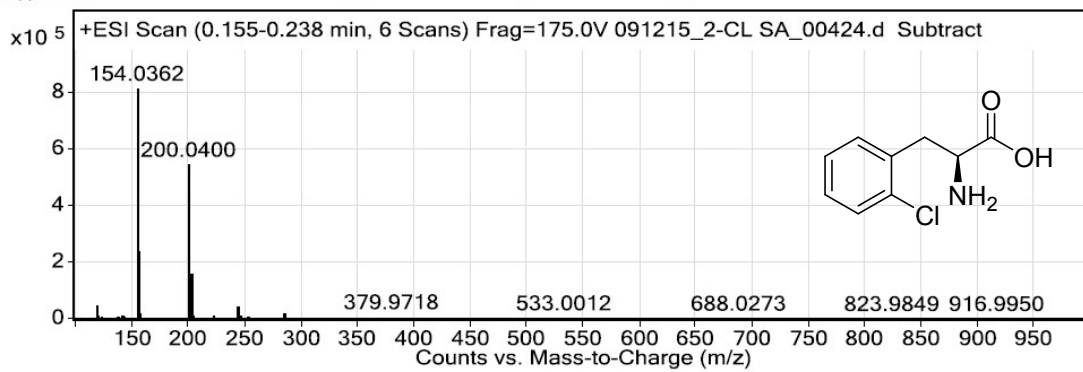


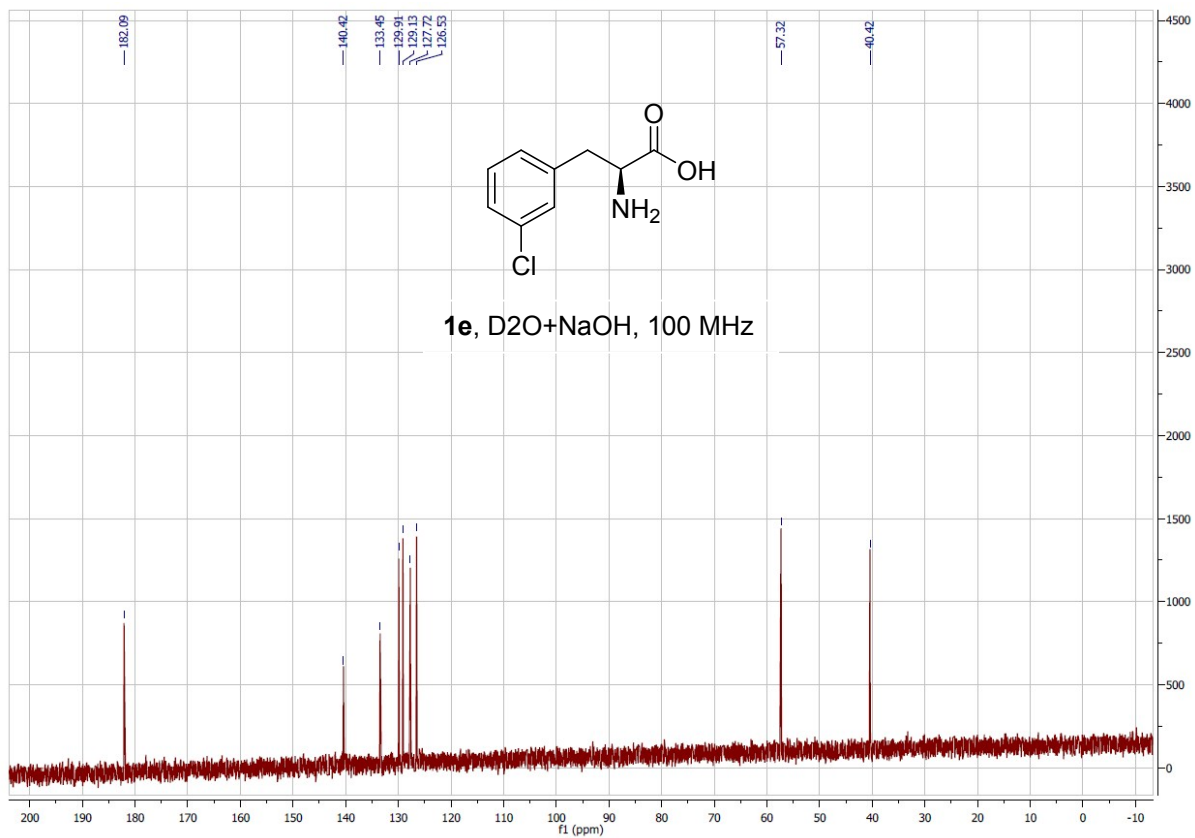
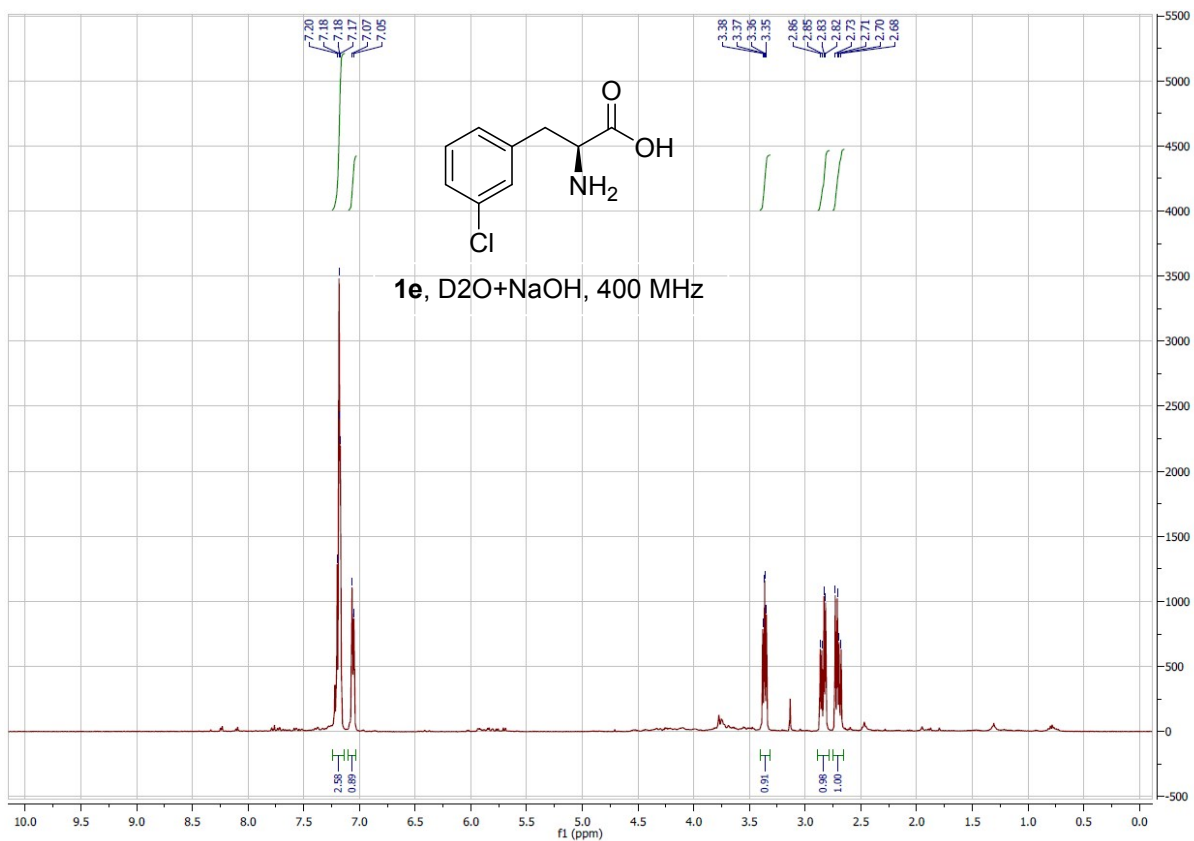
Spectrum Source  
Peak (1) in "+ TIC Scan Smo"

Fragmentor Voltage  
175

Collision Energy  
0

Ionization Mode  
ESI



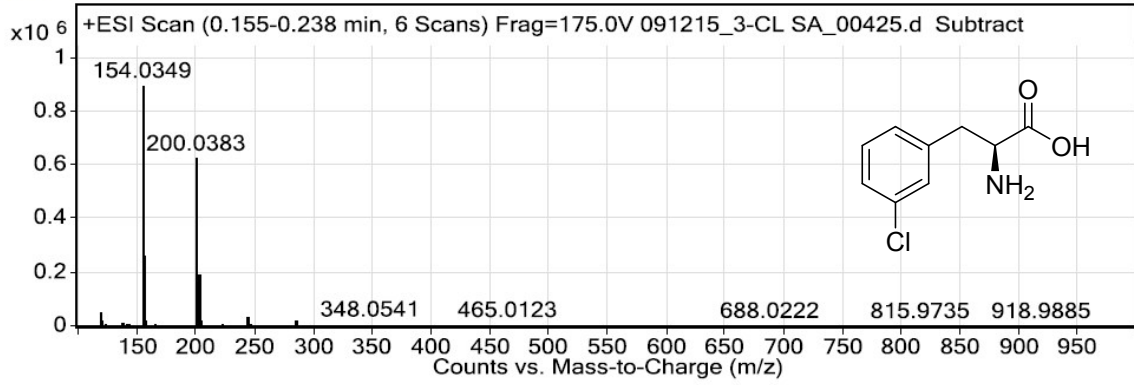


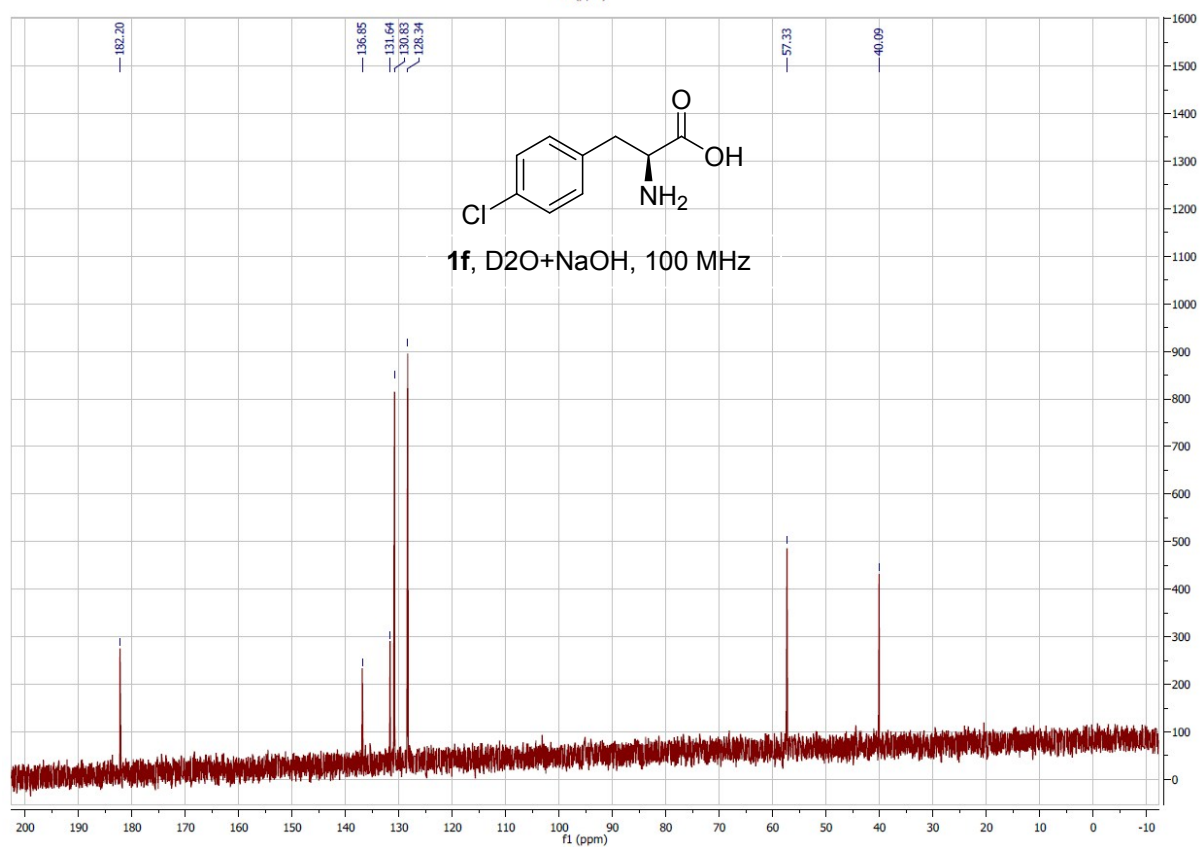
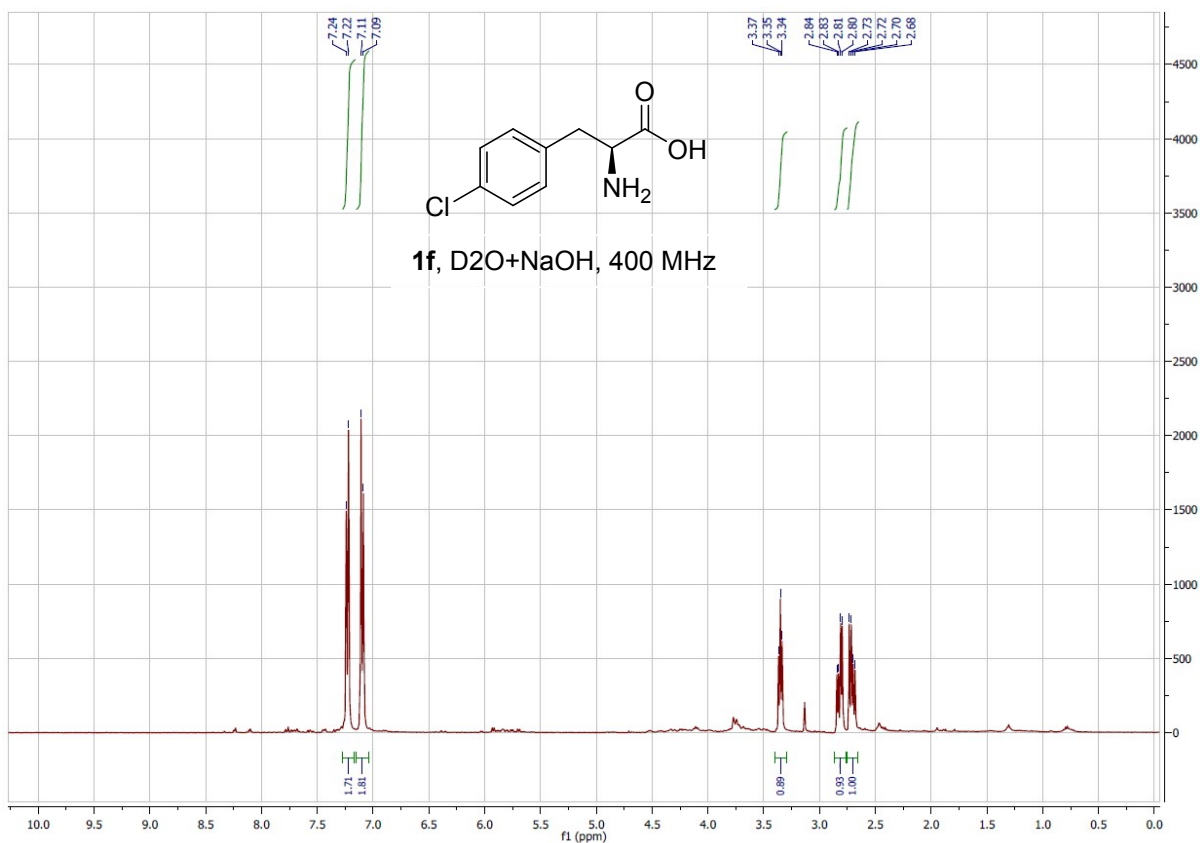
Spectrum Source  
Peak (1) in "TIC Scan Smo"

Fragmentor Voltage  
175

Collision Energy  
0

Ionization Mode  
ESI



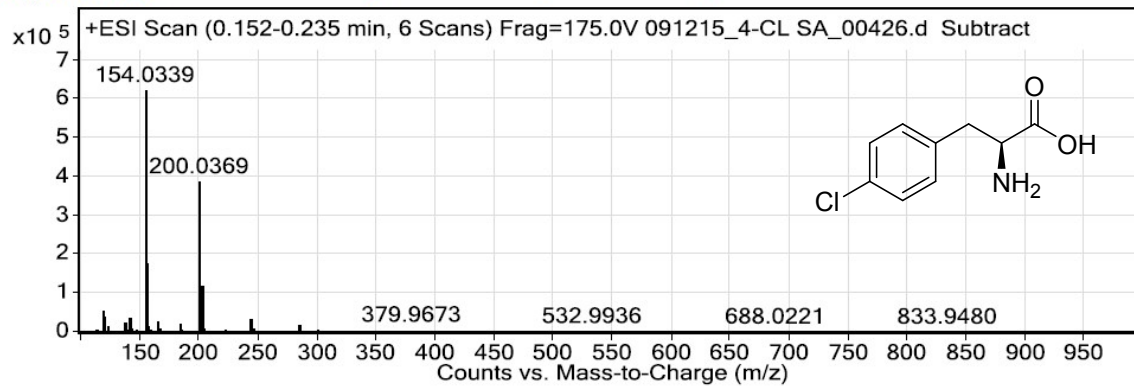


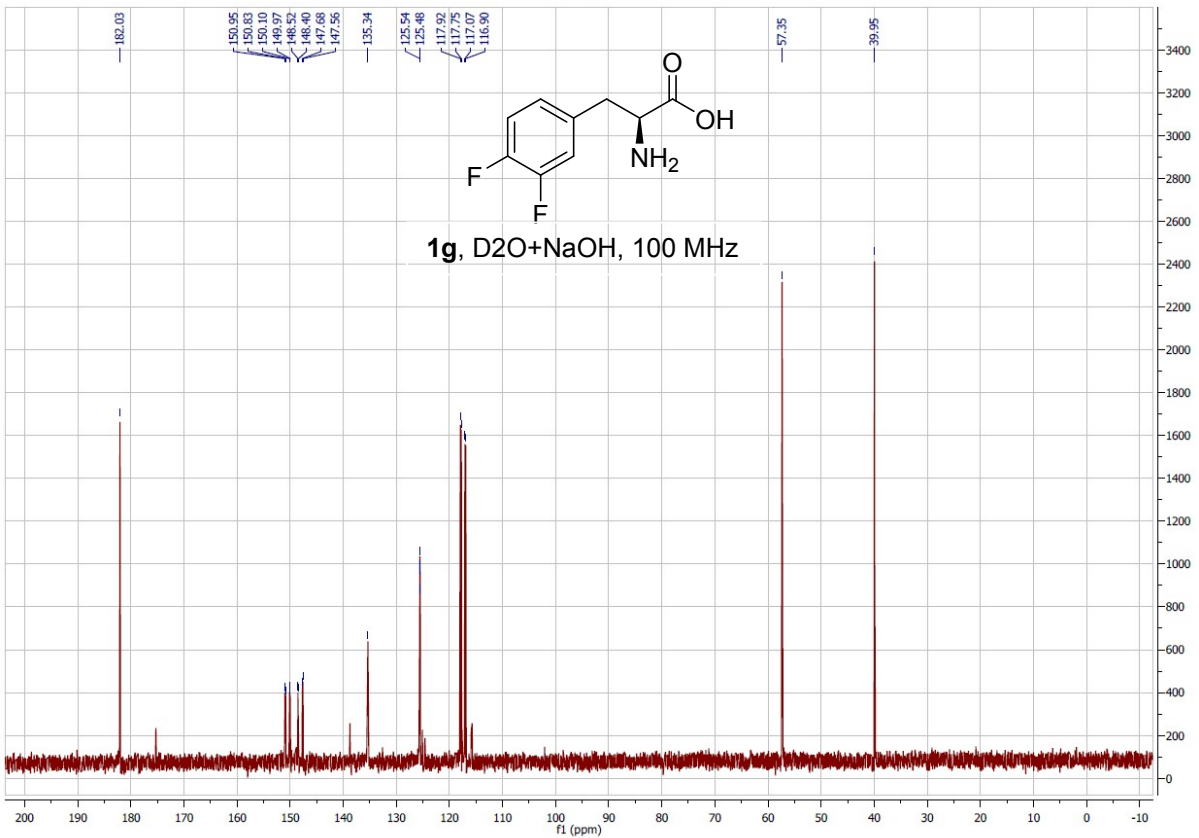
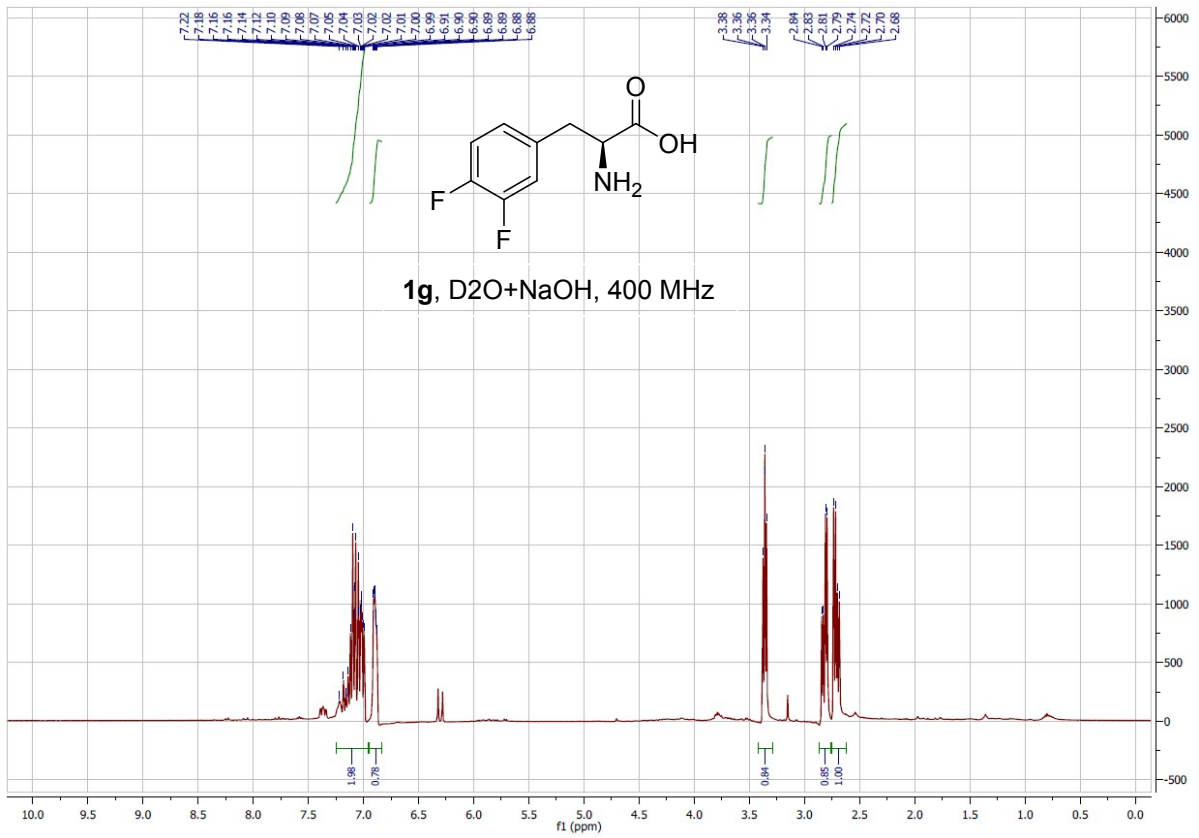
Spectrum Source  
Peak (1) in "+ TIC Scan 5mo"

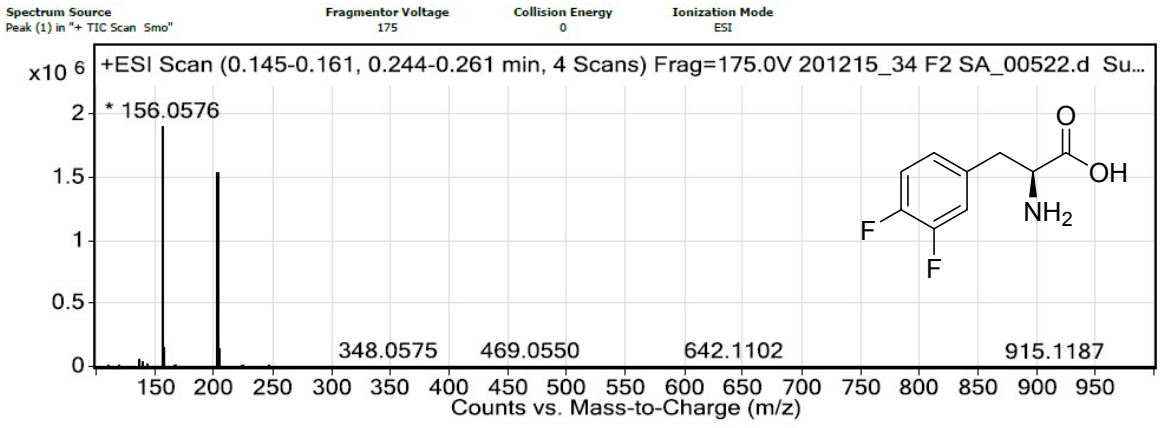
Fragmentor Voltage  
175

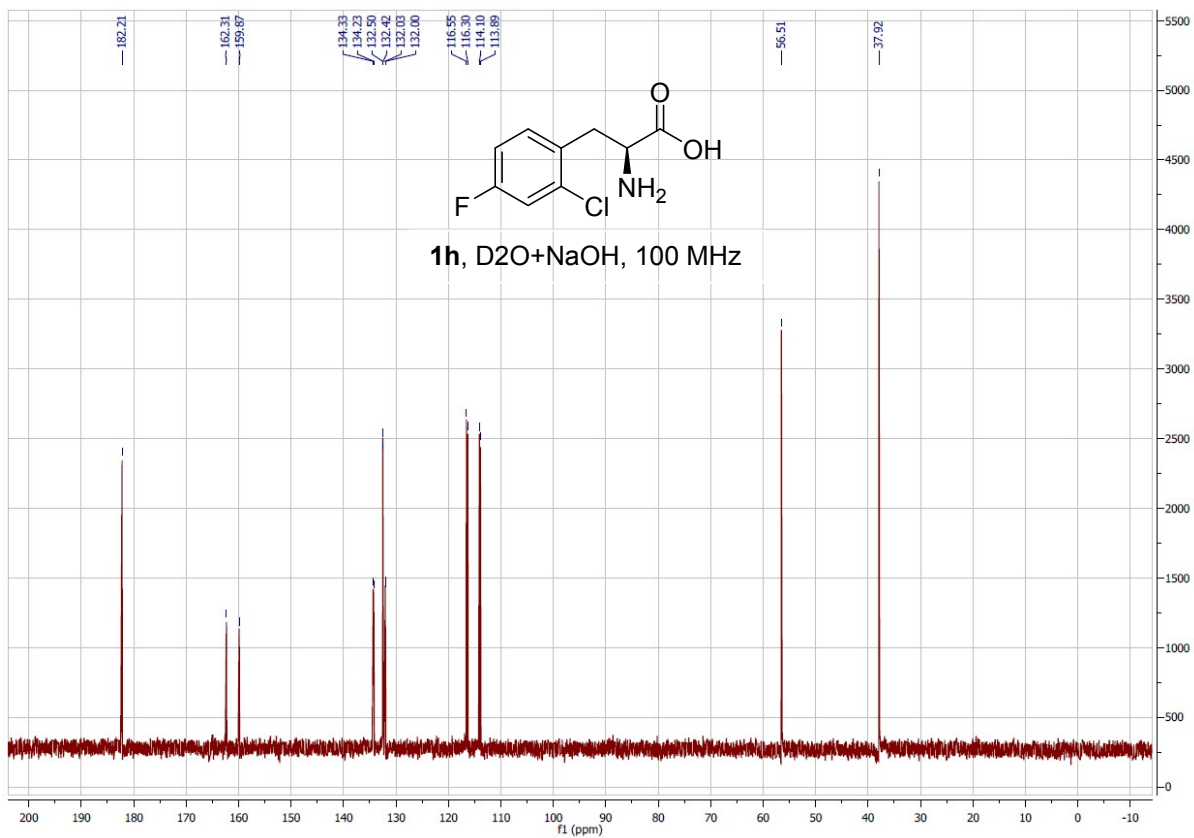
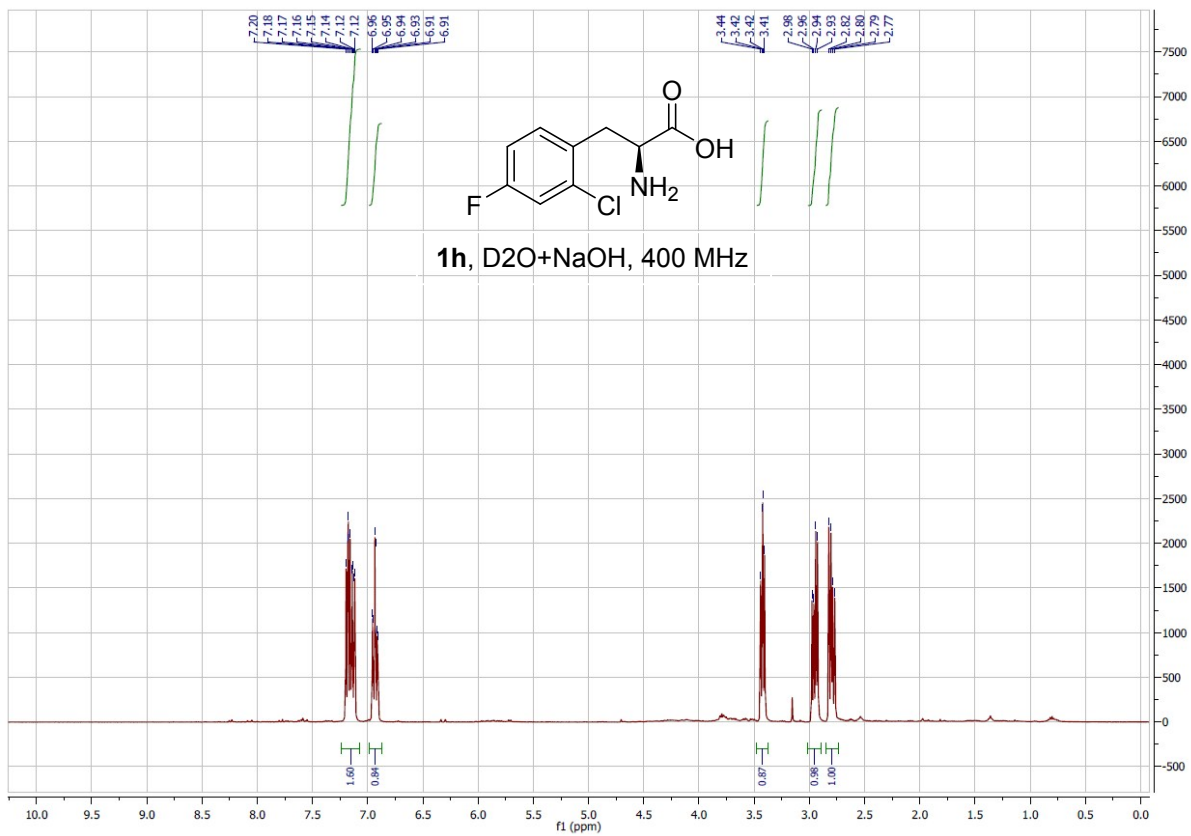
Collision Energy  
0

Ionization Mode  
ESI







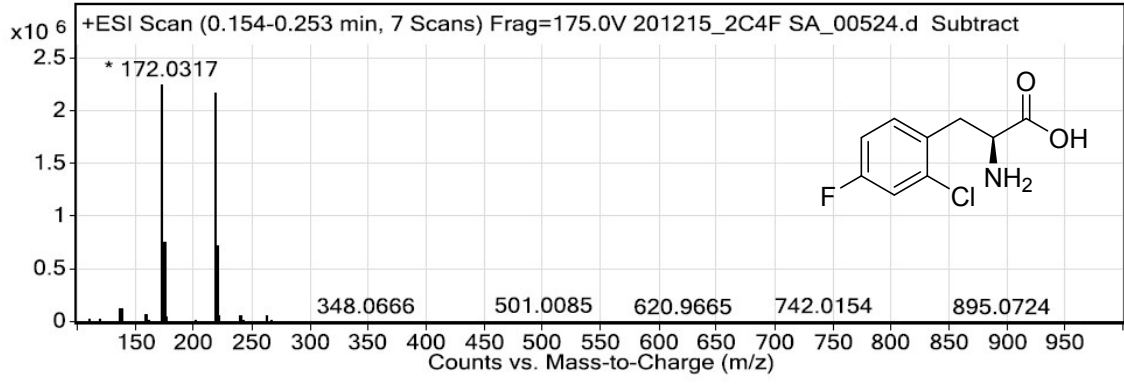


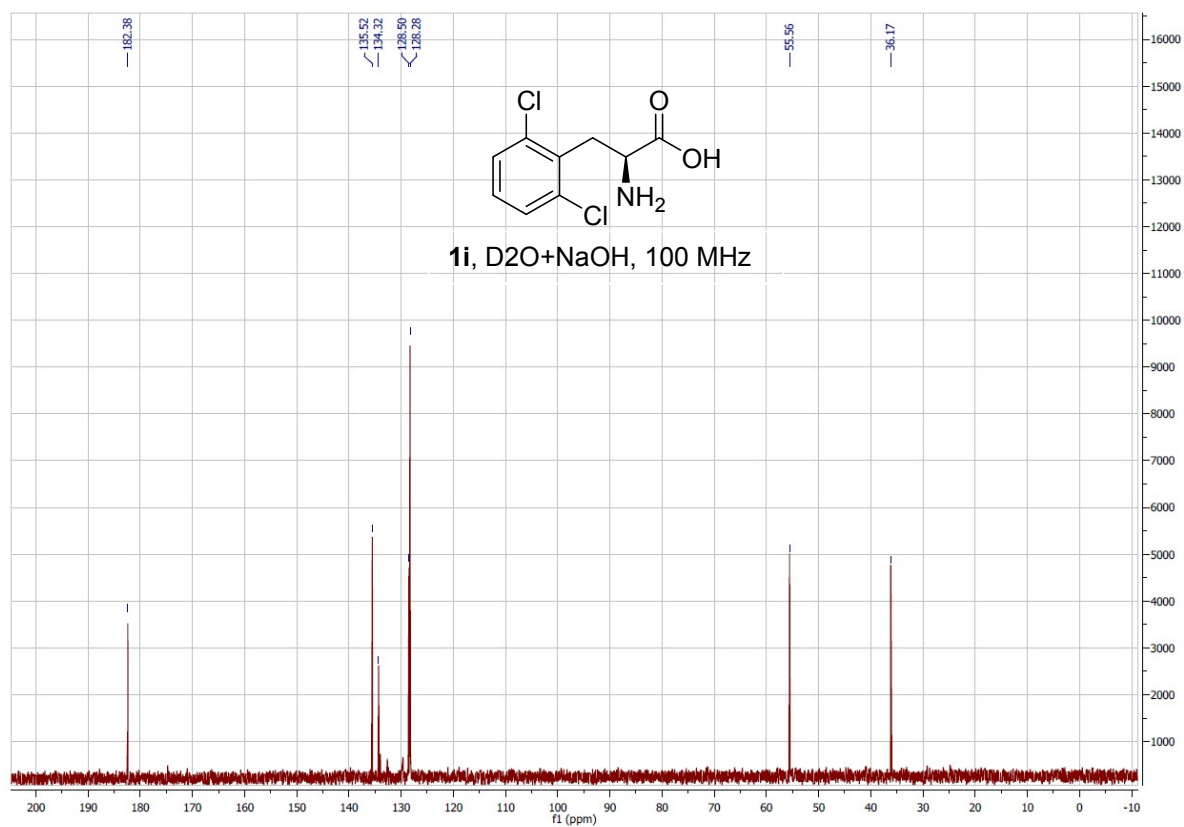
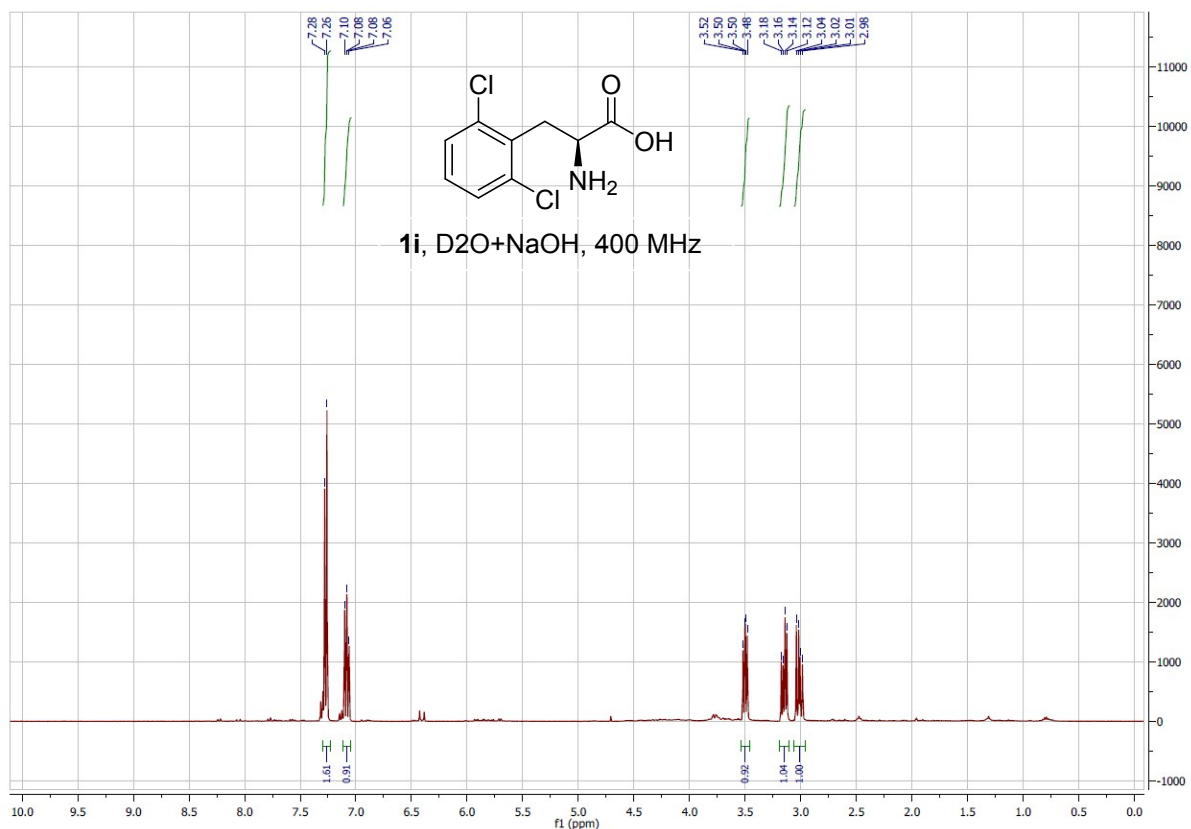
Spectrum Source  
Peak (1) in "TIC Scan Smo"

Fragmentor Voltage  
175

Collision Energy  
0

Ionization Mode  
ESI



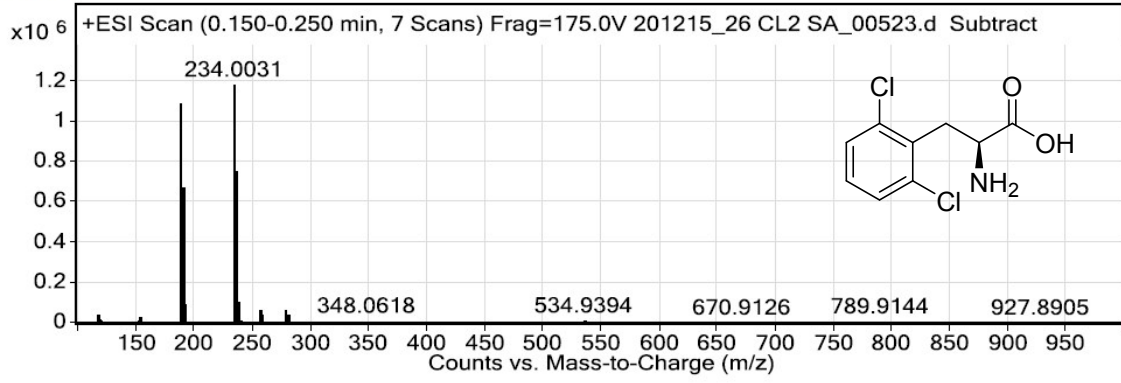


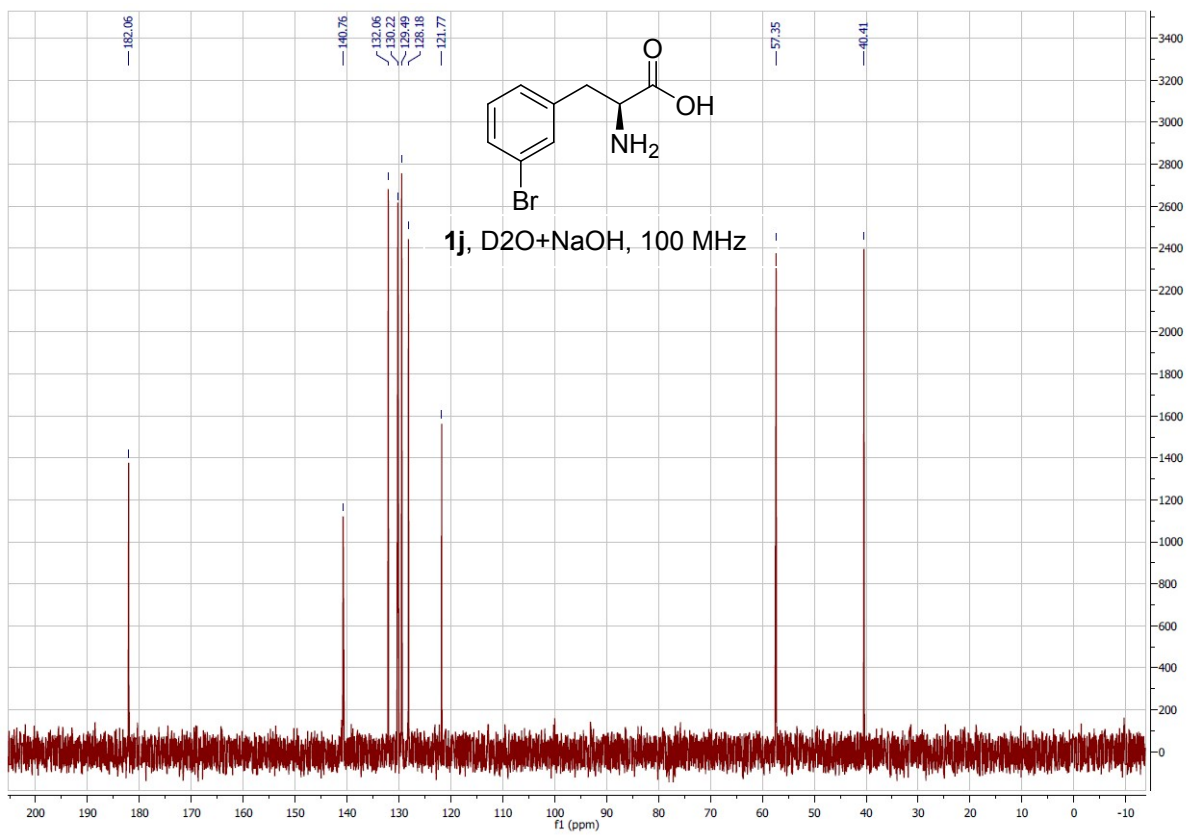
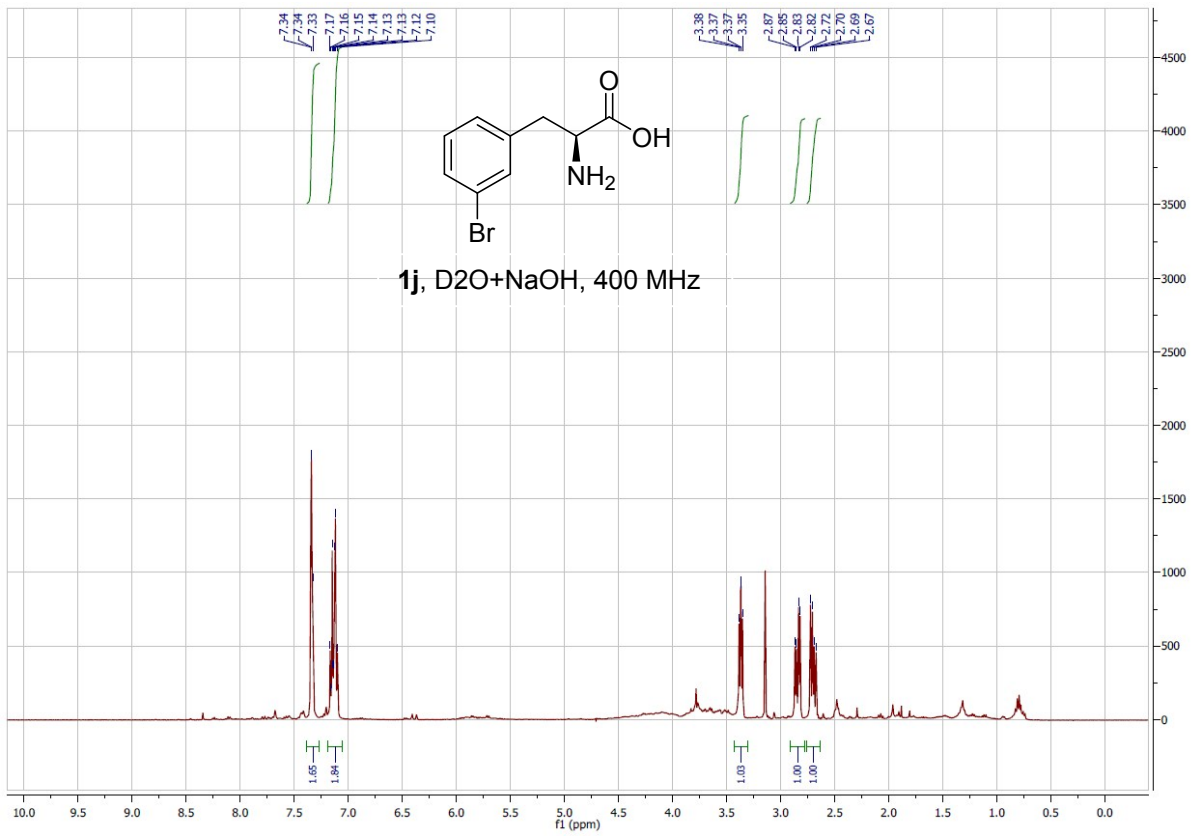
Spectrum Source  
Peak (1) in "+ TIC Scan 5mo"

Fragmentor Voltage  
175

Collision Energy  
0

Ionization Mode  
ESI



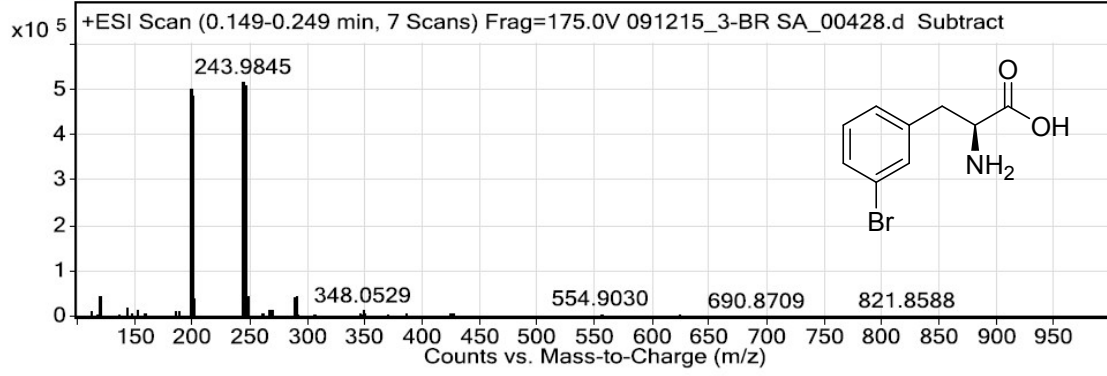


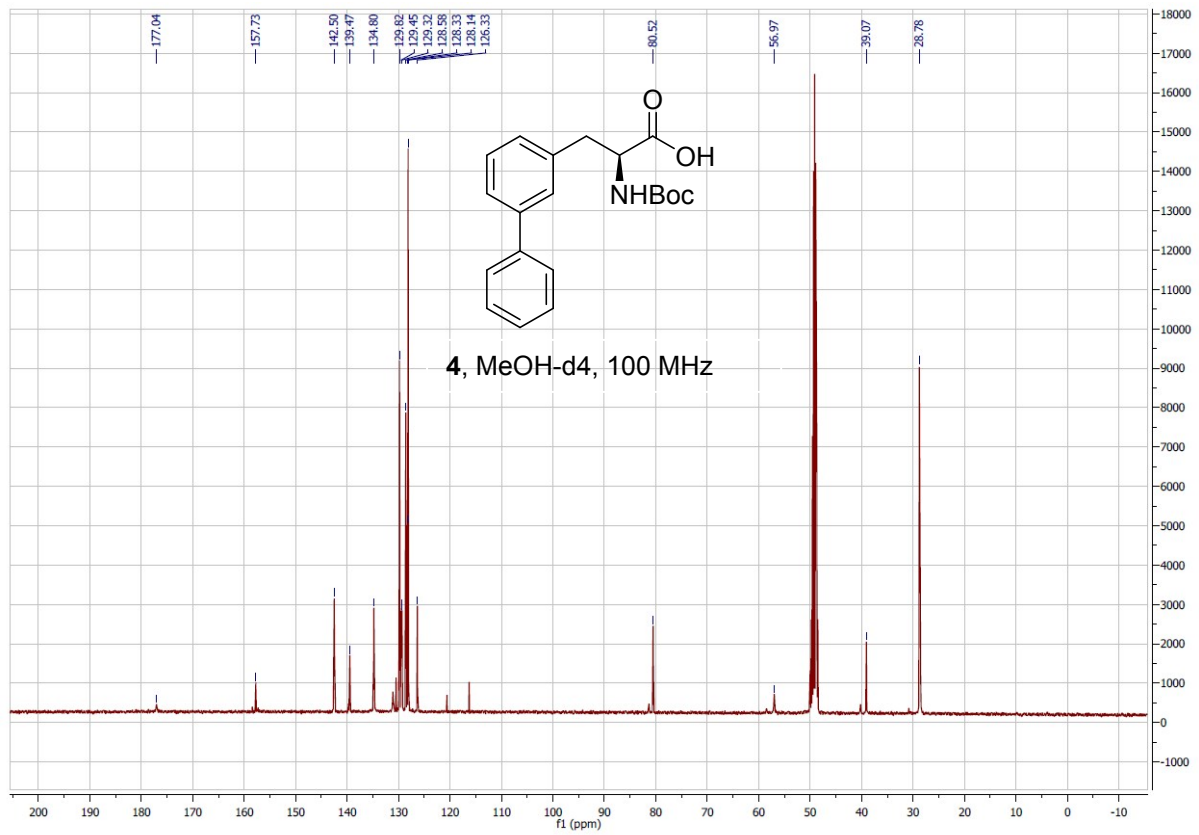
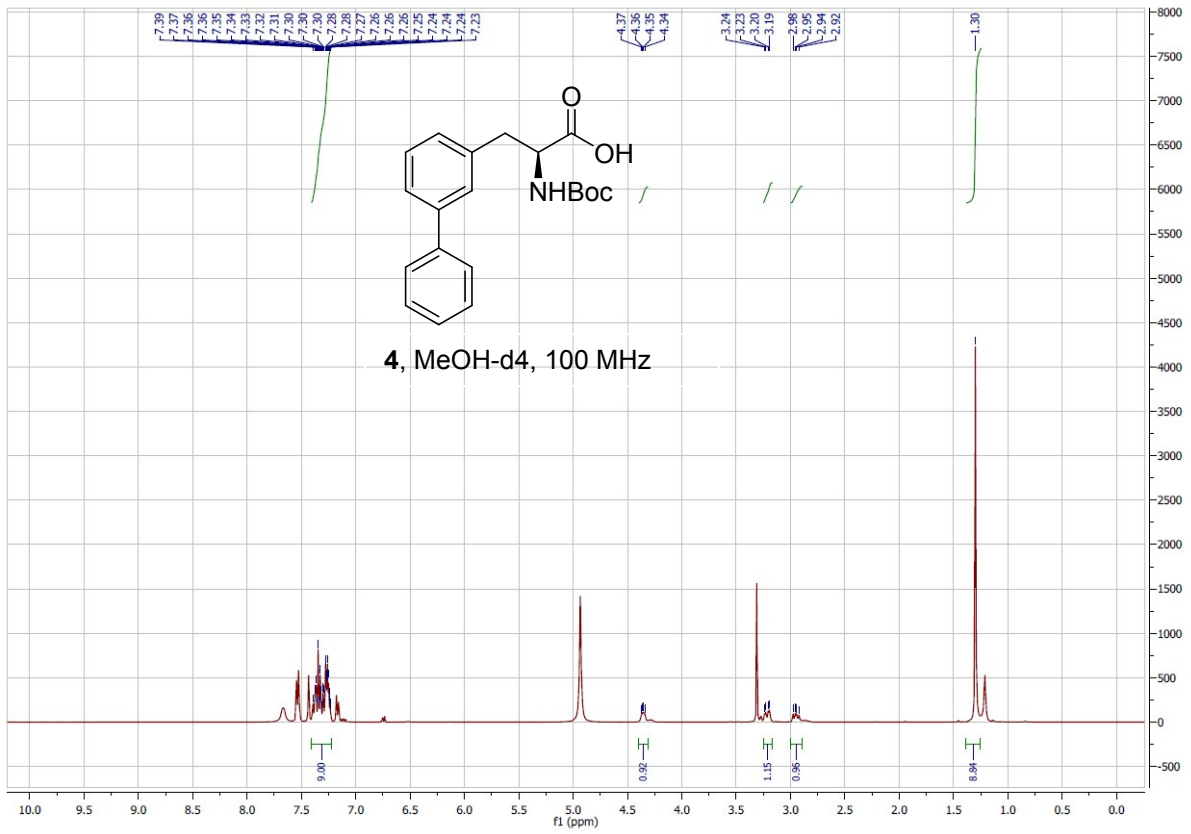
Spectrum Source  
Peak (1) in "+ TIC Scan 5mo"

Fragmentor Voltage  
175

Collision Energy  
0

Ionization Mode  
ESI



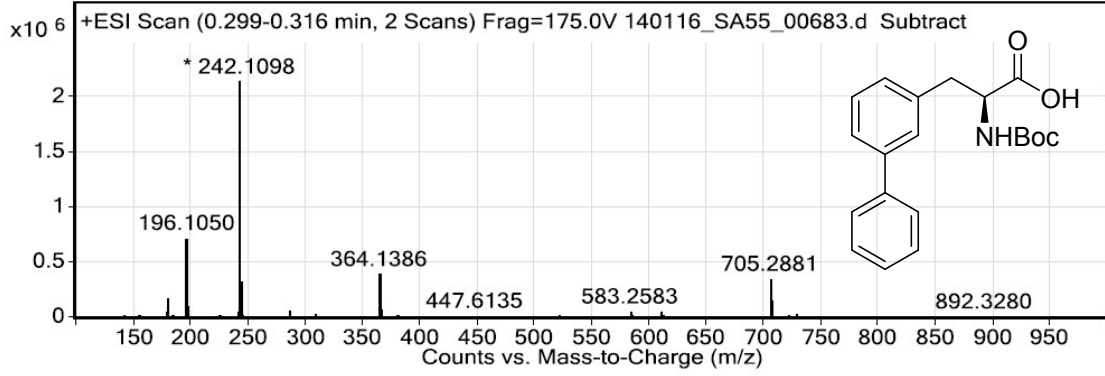


Spectrum Source  
Peak (1) in "+ TIC Scan 5mo"

Fragmentor Voltage  
175

Collision Energy  
0

Ionization Mode  
ESI



## References

- S1 F. Parmeggiani, S. T. Ahmed, N. J. Weise and N. J. Turner, *Tetrahedron*, 2015. DOI: 10.1016/j.tet.2015.12.063
- S2 S. T. Ahmed, F. Parmeggiani, N. J. Weise, S. L. Flitsch and N. J. Turner, *ACS Catal.*, 2015, **5**, 5410–5413.
- S3 A. Gloge, J. Zoń, A. Kövári, L. Poppe and J. Rétey, *Chem. Eur. J.*, 2000, **6**, 3386–90.
- S4 R. A. Sheldon, *Green Chem.*, 2007, **9**, 1273.